

1986

## Formation of Longitudinal Dispersion Coefficient in Partially Mixed Estuaries and Application in a One-Dimensional Real-Time Model

Anne Catherine Wilber  
*College of William and Mary - Virginia Institute of Marine Science*

Follow this and additional works at: <https://scholarworks.wm.edu/etd>

 Part of the [Oceanography Commons](#)

---

### Recommended Citation

Wilber, Anne Catherine, "Formation of Longitudinal Dispersion Coefficient in Partially Mixed Estuaries and Application in a One-Dimensional Real-Time Model" (1986). *Dissertations, Theses, and Masters Projects*. Paper 1539617571.

<https://dx.doi.org/doi:10.25773/v5-tnww-pp09>

This Thesis is brought to you for free and open access by the Theses, Dissertations, & Master Projects at W&M ScholarWorks. It has been accepted for inclusion in Dissertations, Theses, and Masters Projects by an authorized administrator of W&M ScholarWorks. For more information, please contact [scholarworks@wm.edu](mailto:scholarworks@wm.edu).

**FORMULATION OF LONGITUDINAL DISPERSION COEFFICIENT IN  
PARTIALLY MIXED ESTUARIES  
AND  
APPLICATION IN A ONE-DIMENSIONAL REAL-TIME MODEL**

-----  
**A Thesis**

**Presented to**

**The Faculty of the School of Marine Science  
The College of William and Mary in Virginia**

**In Partial Fulfillment**

**Of the Requirements for the Degree of  
Master of Arts**

-----  
**by**

**Anne C. Wilber**

**1986**

ProQuest Number: 10626621

All rights reserved

INFORMATION TO ALL USERS

The quality of this reproduction is dependent upon the quality of the copy submitted.

In the unlikely event that the author did not send a complete manuscript and there are missing pages, these will be noted. Also, if material had to be removed, a note will indicate the deletion.



ProQuest 10626621

Published by ProQuest LLC (2017). Copyright of the Dissertation is held by the Author.

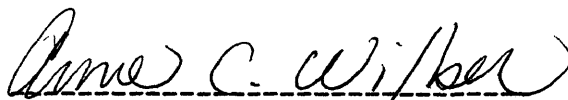
All rights reserved.

This work is protected against unauthorized copying under Title 17, United States Code  
Microform Edition © ProQuest LLC.

ProQuest LLC.  
789 East Eisenhower Parkway  
P.O. Box 1346  
Ann Arbor, MI 48106 - 1346

APPROVAL SHEET

This thesis is submitted in partial fulfillment of  
the requirements for the degree of  
Master of Arts in Marine Science



Anne C. Wilber

Approved, April 1986



Bruce J. Neilson



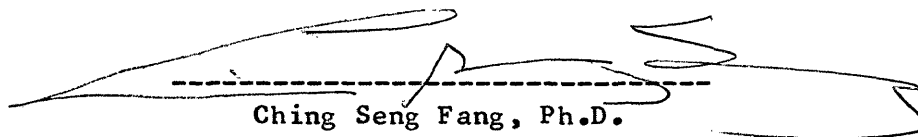
Albert Y. Kuo, Ph.D.



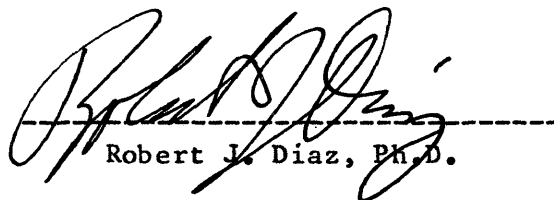
Paul V. Hyer, Ph.D.



Evon P. Ruzecki, Ph.D.



Ching Seng Fang, Ph.D.



Robert J. Diaz, Ph.D.

## **DEDICATION**

**Dedicated to my Family who supported me in many ways throughout the process of this study.**

## TABLE OF CONTENTS

	PAGE
ACKNOWLEDGEMENTS.....	v
LIST OF TABLES.....	vi
LIST OF FIGURES.....	vii
ABSTRACT.....	viii
CHAPTER I. INTRODUCTION.....	2
CHAPTER II. REVIEW OF PREVIOUS INVESTIGATIONS.....	4
CHAPTER III. FORMULATION OF MODEL	
A. Introduction.....	9
B. Basic Equations.....	11
C. Formulation of Dispersion Coefficient.....	14
D. Method of Solution.....	27
E. Boundary and Initial Conditions	
1. Upstream boundary conditions.....	28
a. Dynamic condition.....	28
b. Salinity condition.....	28
2. Downstream boundary conditions	
a. Dynamic condition.....	28
b. Salinity condition.....	29
3. Initial conditions	
a. Dynamic condition.....	30
b. Salinity condition.....	30
F. Comparison of Model with Analytical Solution.....	31
CHAPTER IV. APPLICATION TO THE RAPPAHANNOCK	
A. Model Set-Up.....	35
B. Hydrodynamic Calibration.....	40
C. Salinity Calibration.....	55
D. Role of Gravitational Circulation and Stratification in the Dispersion Coefficient .....	65
CHAPTER V. SUMMARY AND CONCLUSIONS.....	70
APPENDIX.....	74
LITERATURE CITED.....	81
VITA.....	85

## **ACKNOWLEDGEMENTS**

**The author wishes to express her appreciation to the members of her committee and to the students and staff of the Department of Physical Oceanography and Environmental Engineering for their help and support. Special thanks are extended to Dr. Albert Y. Kuo for his patient guidance during this investigation.**

## LIST OF TABLES

TABLE	PAGE
1. GEOMETRIC DATA.....	39
2. HARMONIC CONSTANTS.....	43
3. DISPERSION COEFFICIENTS.....	68
4. RICHARDSON NUMBERS.....	69



## LIST OF FIGURES

FIGURE	PAGE
3-1 Comparison with Analytical Solution.....	34
4-1 Segmentation of River.....	38
4-2 Mean Tide Range.....	44
4-3 Time of High Tide.....	45
4-4 Time of Low Tide.....	46
4-5 Time of Ebb.....	47
4-6 Time of Flood.....	48
4-7 Time of Slack Before Ebb.....	49
4-8 Time of Slack Before Flood.....	50
4-9 Predicted Surface at Windmill Point July 1973.....	51
4-10 Freshwater Inflow.....	52
4-11 Current at Windmill Point.....	53
4-12 Current at Grey Point.....	54
4-13 Salinity Distribution May 31, 1973.....	58
4-14 Salinity Distribution July 11, 1973.....	59
4-15 Salinity Distribution August 8, 1973.....	60
4-16 Salinity Distribution September 26, 1973.....	61
4-17 Salinity Distribution October 30, 1973.....	62
4-18 Salinity at Windmill Point.....	63
4-19 Salinity at Grey Point.....	64

## ABSTRACT

Salinity distribution is an important factor in water quality. It is also the forcing function for gravitational circulation. A one-dimensional, real-time, hydrodynamic and salinity intrusion model was applied to an estuary in order to predict the longitudinal salinity distribution. It was necessary to formulate a dispersion coefficient to account for the effect of gravitational circulation in the saline portion of the estuary.

The model is based on the one-dimensional equations of conservation of volume, momentum and mass. The estuary was divided into segments and a semi-implicit finite difference scheme was used to solve the governing equations.

The dispersion was formulated to consist of three terms. The first is the dispersion due to the effects of vertical shear of the tidal flow, the second is dispersion due to the effects of transverse shear of the tidal flow, and the third is dispersion due to the effects of gravitational circulation. The first two terms are based on Taylor's analysis of flow and are applicable in the freshwater portion of the estuary. The third term was formulated based on the analysis of Hansen and Rattray (1965). The dispersion due to gravitational circulation is found to depend on the local hydraulic conditions and the local longitudinal salinity gradient.

The model was calibrated and verified using slack water and intensive survey data from the Rappahannock River. The longitudinal salinity distribution was simulated from March through October 1973.

During this time the freshwater inflow varied from 11 to 450 m<sup>3</sup>/sec. The inputs necessary to successfully predict both short-term and long-term salinity variations are the freshwater inflow, the time varying surface elevation and the salinity at the mouth.

**FORMULATION OF A LONGITUDINAL DISPERSION COEFFICIENT IN PARTIALLY-MIXED  
ESTUARIES AND APPLICATION IN A ONE-DIMENSIONAL REAL-TIME MODEL**

## I. INTRODUCTION

An estuary has been defined as a partially enclosed body of water which has free access to the open sea and within which sea water is measurably diluted with fresh water from the land (Pritchard 1952). Salinity is a distinguishing property of an estuary. Density gradients are a characteristic of estuaries which cause gravitational circulation, which in turn is a dominant influence on transport of momentum, and dissolved and suspended pollutants. In estuaries the density field is determined by salinity distribution. The variation of salinity distribution on an estuary determines the extreme conditions sedentary organisms are subject to, and the distribution of plankton and nekton. The location of the head of the intrusion is important to communities drawing their water supply from the tidal river. Once the hydrodynamics and salinity distribution have been modeled the model can be used to predict distribution of other water quality parameters.

The salinity distribution is determined by meteorological effects, tidal motions, river flow, channel geometry and bed roughness. These factors make a quantitative description of salinity and dispersion difficult. The research on dispersion has been motivated by the practical importance of gravitational circulation and salinity distribution. Mathematical models are used to describe dispersion. Many different kinds of models are currently being developed and used.

A mathematical model uses equations to describe important physical processes which occur in real estuaries. This study presents a predictive numerical model of unsteady salinity intrusion in an estuary by using the one-dimensional, real time equations for the conservation of water mass, conservation of momentum and conservation of salt. A dispersion coefficient is formulated for use in the model.

## II. REVIEW OF PREVIOUS INVESTIGATIONS

The first attempts to model substance concentrations in estuaries were zero dimensional. The estuary was treated as a homogeneous body of water. The water entering on flood tide was assumed to be completely mixed with the water inside the estuary. The volume of sea water and river water introduced equals the volume of the tidal prism, the difference in estuarine volume between high and low tide. This model is known as the tidal prism model. This approach is valid only for small coastal embayments.

Ketchum (1951) modified the tidal prism model by dividing the estuary into segments whose lengths were equal to the local tidal excursion. Within each segment complete mixing is assumed. This model is useful for calculating flushing time and salinity distribution knowing only the river flow and tidal range in an estuary. It has been applied to the Raritan River and the Bay of Fundy with reasonably good agreement with the salinity distribution. For other estuaries the agreement was not good. The model works best in well mixed estuaries. Therefore it is not applicable to the partially-mixed estuaries common to the East coast of North America.

Arons and Stommel (1951) modified Ketchum's concept and derived the longitudinal salinity distribution:  $S = S_0 \exp[F(1-L/x)]$  in which  $S_0$  is the salinity outside the mouth,  $F$  is an empirical flushing number,  $L$  is the length of the salinity intrusion, and  $x$  is distance measured from the head. The results are applicable only to steady-state studies of estuaries which can be approximated by a constant rectangular cross section.

Dyer and Taylor (1973) proposed a more general approach to the tidal prism model. Their model allows for additional inflows from tributaries and outfalls and incorporates a parameter associated with mixing. The model was successfully applied to the Raritan River and the Thames.

Ketchum's model segmented the estuary from the head down using river flow to start the segmentation. Kuo (1976) segmented the estuary from the mouth upriver. This enables an estuary with negligible fresh water inflow to be modeled. The model is applicable to small coastal embayments that are well-mixed where the tidal exchange is the only flushing mechanism.

Wood (1979) combined aspects of the models by Ketchum, Dyer and Taylor. Wood bases the segmentation on complete displacement during ebb-flow where Ketchum used flood-tide displacements. This model also contains exchanges between segments as a result of mixing as in the Dyer and Taylor model.

Steady-state analyses are limited to conditions in which an estuary approaches a steady-state. This requires that both ocean tidal ranges and fresh water inflow remain relatively constant for at least a month for most estuaries. The dispersion relationship obtained is valid for the conditions of fresh water discharge and tidal range for which the data was taken, extrapolation to other conditions is not justifiable without more data.

Another one-dimensional approach used by Okubo (1964), Holley and Harleman (1965) employs the mass-balance equation derived by spatial

integration of the three-dimensional equation over the flow cross-section. The basic assumption inherent in one-dimensional models is that vertical and lateral differences are negligible.

Models differ in the handling of time scales. Tidal average and slack tide models have been formulated, (Pritchard 1959, Boicourt 1969). In these models the mass-balance equation is averaged over a time period equal to a tidal cycle. This results in the advection term containing the fresh water discharge rather than the instantaneous discharge. The cross-sectional area is no longer a function of time. The dispersion coefficient includes the effects of the time averaging process. The models are useful in economically representing long term changes in concentration but ignore intratidal variations.

A tidal-time or real-time model refers to a time scale much less than that of a tidal cycle but greater than that defining turbulence. Thatcher and Harleman (1972) developed a predictive model of salinity by developing a numerical solution to the one-dimensional salt balance and tidal dynamics equations. The equations are coupled through an equation of state relating salinity to density. The tidal-time approach enables the prediction of the range of salinity concentration during a tidal cycle as well as the average concentration.

In practice the simplest model that can solve the problem should be the one to use. One-dimensional models are often the choice because they are economical and can model several parameters sufficiently accurately. Estuaries are three-dimensional and the more dimensions used the better velocities and concentration are represented. In some situations multi-dimensional models are desirable.

When applying a two-dimensional model a choice must be made whether to average over the vertical or lateral dimension. Leendertse (1973)



developed a two-dimensional vertically integrated model that represents tidal current, wind driven, and Coriolis circulations and dispersion mechanisms of trapping and pumping. The model includes non-linear friction and inertial terms. It was applied to Jamaica Bay with good results. The model works well on small vertically well-mixed water bodies. It takes a lot of computer time for the model to reach equilibrium.

Hamilton (1975) developed a time dependent multi-level two-dimensional model of vertical circulation using explicit finite difference solutions to the continuity, salt and momentum equations in a rectangular channel of variable width and depth. The model was applied to the Rotterdam Waterway resulting in agreement with field observations of salinity distribution and current.

Hamilton (1977) revised his model using a semi-implicit numerical scheme which allowed for longer time steps between calculation, therefore resulting in savings in computer time. The model was applied to a hypothetical channel to study the effect on the salt balance of different formulations of vertical eddy coefficients.

Blumberg (1975) solved the continuity, salt and momentum equations using a leap-frog finite-difference scheme. The model is in real time and assumes a laterally homogeneous estuary with realistic bathymetry. In applications to the Potomac River the salinity distribution was found to be comparable to field observations. The model shows salinity intrusion to be highly sensitive to vertical eddy viscosity.

Kuo et al (1978) applied a two-dimensional laterally average, real time model to simulate movement of water and suspended sediment in the

turbidity maximum. The model was applied to the Rappahannock River with good results.

Wang and Kravitz (1980) applied a semi-implicit, laterally averaged model to the Potomac to simulate tidal, wind and density driven circulations. The model became the base for a branching model for application to complex estuaries (Wang 1983). In application to the Chesapeake Bay there was good agreement for the depth averaged salinity distribution during a period of low flow from the Susquehanna River. The extent of the salinity intrusion in the model is dependent on parameterization of vertical mixing and friction.

Festa and Hansen (1976) used a steady state, non-tidal, laterally averaged model to investigate the effects of altering the river depth and fresh water inflow on estuarine circulation and salinity. They found that decreasing river flow allowed the head of the salinity intrusion to move upstream. An increase in flow strengthened gravitational circulation. Increasing the river depth enhanced the circulation and resulted in movement of the salinity intrusion upstream.

Cerco (1982) developed a two-dimensional laterally averaged model for partially mixed estuaries to make intra-tidal predictions of surface level, velocity and salinity. The model was used to simulate the destratification-stratification cycle that is coincident with the spring-neap tidal cycle in the James River. The movement of the salinity intrusion following a storm generated fresh water inflow pulse, was also modeled.

### **III. FORMULATION OF MODEL**

#### **A. Introduction**

A mathematical model of salt intrusion is based on equations that describe physical processes that occur in real estuaries. Simplification and assumptions are made and the model is calibrated and verified using field observations. After verification the model can be used to predict changes in the dynamics and salinity with changes in the input parameters.

Equations in three dimensions are needed to completely describe the dynamics and salinity distribution. Three-dimensional models are not yet practical and consume large amounts of computer time. An estuary is often elongate and lateral variations can be considered of secondary importance. In a partially mixed estuary there is vertical variation in salinity but a one-dimensional model can predict the longitudinal distribution of salinity accurately. Therefore a one-dimensional model is chosen for this study because it is economical and sufficiently accurate for the purpose of predicting salinity intrusion. Because there is great temporal variability in the parameters affecting salinity, a real-time model is necessary to predict salinity distribution.

The salinity distribution is governed principally by the geometry of the estuary, the time history of fresh water inflow and the tidal dynamics. This study presents a predictive model of salinity intrusion by using the one-dimensional hydrodynamic and salt balance equations. The freshwater inflow and surface elevation at the mouth are inputs to the model.

## B. Basic Equations

The derivation of unsteady continuity and momentum equations has been made by many investigators, Harleman and Lee (1969) and Harleman (1971). The three-dimensional equations used for describing hydrodynamics and salt balance in an incompressible flow may be written as:

the continuity equation

$$\frac{\delta u}{\delta x} + \frac{\delta v}{\delta y} + \frac{\delta w}{\delta z} = 0 \quad (3-1)$$

the momentum equations

$$\begin{aligned} \frac{\delta u}{\delta t} + u \frac{\delta u}{\delta x} + v \frac{\delta u}{\delta y} + w \frac{\delta u}{\delta z} = & -\frac{1}{\rho} \frac{\delta P}{\delta x} + \nu \nabla^2 u + \frac{\delta}{\delta x} (\overline{-u'^2}) \\ & + \frac{\delta}{\delta y} (\overline{-u'v'}) + \frac{\delta}{\delta z} (\overline{-u'w'}) \end{aligned} \quad (3-2)$$

$$\begin{aligned} \frac{\delta v}{\delta t} + u \frac{\delta v}{\delta x} + v \frac{\delta v}{\delta y} + w \frac{\delta v}{\delta z} = & -\frac{1}{\rho} \frac{\delta P}{\delta y} + \nu \nabla^2 v + \frac{\delta}{\delta x} (\overline{-u'v'}) \\ & + \frac{\delta}{\delta y} (\overline{-v'^2}) + \frac{\delta}{\delta z} (\overline{-v'w'}) \end{aligned} \quad (3-3)$$

$$\begin{aligned} \frac{\delta w}{\delta t} + u \frac{\delta w}{\delta x} + v \frac{\delta w}{\delta y} + w \frac{\delta w}{\delta z} = & -\frac{1}{\rho} \frac{\delta P}{\delta z} - g + \nu \nabla^2 w + \frac{\delta}{\delta x} (\overline{-u'w'}) \\ & + \frac{\delta}{\delta y} (\overline{-v'w'}) + \frac{\delta}{\delta z} (\overline{-w'^2}) \end{aligned} \quad (3-4)$$

the salt balance equation

$$\begin{aligned} \frac{\delta s}{\delta t} + u \frac{\delta s}{\delta x} + v \frac{\delta s}{\delta y} + w \frac{\delta s}{\delta z} = & \frac{\delta}{\delta x} (\overline{-u's'}) + \frac{\delta}{\delta y} (\overline{-v's'}) \\ & + \frac{\delta}{\delta z} (\overline{-w's'}) + \varepsilon \nabla^2 s \end{aligned} \quad (3-5)$$

where  $t$  is time,  $u$ ,  $v$  and  $w$  are the ensemble average velocity components in the  $x$ ,  $y$  and  $z$  directions respectively,  $u'$ ,  $v'$  and  $w'$  are the turbulent velocity fluctuations,  $P$  is the pressure,  $g$  is gravitational acceleration,  $\rho$  is the water density,  $\nu$  is the kinematic viscosity,  $\nabla^2$

is the Laplacian operator,  $s$  is the ensemble average salinity,  $s'$  is the turbulent salinity fluctuation, and  $\epsilon$  is the molecular diffusion coefficient. In practical application ensemble averages are replaced by time averages over an interval longer than the turbulent time scale but much shorter than a tidal cycle.

Integrating the three-dimensional hydrodynamic equations over a cross section normal to the axis of the estuary yields the one-dimensional equations. (Williams and Kuo 1984)

The continuity equation

$$B \frac{\delta \eta}{\delta t} + \frac{\delta Q}{\delta x} - q = 0 \quad (3-6)$$

The momentum equation

$$\frac{\delta Q}{\delta t} + \frac{\delta}{\delta x} \left( \frac{Q^2}{A} \right) = -gA \frac{\delta \eta}{\delta x} - \frac{gk}{1+ks} Ad \frac{\delta s}{\delta x} - gn \frac{Q|Q|}{A R^{4/3}} + \frac{\tau_s}{\rho} B \quad (3-7)$$

where:

$A$  = the cross sectional area

$B$  = the channel width

$g$  = gravitational acceleration

$Q$  = the cross sectional discharge

$q$  = the lateral inflow per unit length

$R$  = the hydraulic radius

$n$  = Manning's friction coefficient

$\eta$  = the surface elevation relative to mean water level

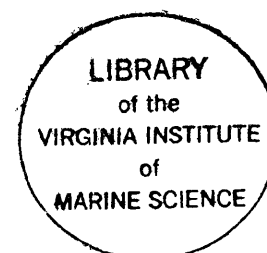
$\tau_s$  = the average wind stress on the water surface

$d_c$  = the distance from the surface to the centroid of the cross section

The equation of state relates water density to salinity. Knudson (1901) developed tables relating density to temperature, pressure, and salinity. In estuaries the effect of pressure on density is assumed to be negligible. The range of temperature in an estuary at any given time is generally narrow, therefore the effect of temperature on density is neglected. In an estuary a more simple relationship can be used:

$$\rho = \rho_0 (1 + ks)$$

where  $\rho_0$  is the density of fresh water in gm/cm<sup>3</sup> and k is a constant found to be 0.00075 when salinity is measured in parts per thousand.



### C. Formulation of Dispersion Coefficient

The three-dimensional salt balance equation has been shown in Equation (3-5).

A turbulent diffusion coefficient can be defined analagous to the molecular diffusion coefficient, the relationship can be written:

$$\overline{-u's'} = e_x \frac{\delta s}{\delta x} \quad (3-8)$$

$$\overline{-v's'} = e_y \frac{\delta s}{\delta y} \quad (3-9)$$

$$\overline{-w's'} = e_z \frac{\delta s}{\delta z} \quad (3-10)$$

where  $e_x, e_y, e_z$  are turbulent diffusion coefficients.

The molecular diffusion can be neglected because the turbulent diffusion coefficients are generally several orders of magnitude greater than the molecular diffusion coefficients. The three-dimensional salt balance equation then becomes:

$$\frac{\delta s}{\delta t} + u \frac{\delta s}{\delta x} + v \frac{\delta s}{\delta y} + w \frac{\delta s}{\delta z} = \frac{\delta}{\delta x} (e_x \frac{\delta s}{\delta x}) + \frac{\delta}{\delta y} (e_y \frac{\delta s}{\delta y}) + \frac{\delta}{\delta z} (e_z \frac{\delta s}{\delta z}) \quad (3-11)$$

The one-dimensional salt balance equation is found by integrating the three-dimensional equation (3-11) over a cross section normal to the axis of the estuary. The time average concentrations and velocity components are defined as:

$$u = U + u'' \quad (3-12)$$

$$v = v''$$

$$w = w''$$

$$s = S + s''$$

where the double primed quantities  $u'', v'', w''$  are spatial deviations of velocity from the cross sectional mean value,  $U = \frac{1}{A} \iint u dA$  is the real



time longitudinal velocity averaged over the cross section,  $S = \frac{1}{A} \iint s dA$  is the salinity averaged over the cross section and  $s''$  is the spatial deviation of the salinity from the average.

Note that  $\iint u'' dA = 0$ , and that  $v''$  and  $w''$  are not zero even though the cross section mean velocities  $V$  and  $W$  are zero in a one-dimensional flow.

The expressions in equation (3-12) are then substituted into equation (3-11) and integrated over the cross section (Holley and Harleman 1965). The resulting equation may be written as:

$$\frac{\delta}{\delta t} (AS) + \frac{\delta}{\delta x} (AUS) = - \frac{\delta}{\delta x} \iint u'' s'' dA + \frac{\delta}{\delta x} (Ae_x \frac{\delta S}{\delta x}) + qS_T \quad (3-13)$$

where  $qS_T$  is the flux of salt through the lateral boundaries and  $S_T$  is the salinity concentration in the lateral flow.

It has been shown (Taylor 1954, Aris 1956) that for steady uniform flow and for  $s''$  much less than  $s$ , the cross section average of  $u'' s''$  is analagous to a dispersive process and can be represented by a longitudinal dispersion coefficient  $E_x$ , which is defined from:

$$\iint u'' s'' dA = -AE_x \frac{\delta S}{\delta x} \quad (3-14)$$

Mass transport is in the direction of decreasing concentration as indicated by the negative sign. Taylor (1954) has shown that  $E_x \gg e_x$ . Therefore it is convenient to define the longitudinal dispersion coefficient as the sum:

$$E = E_x + e_x \quad (3-15)$$

Equation (3-13) becomes:

$$\frac{\delta}{\delta t} (AS) + \frac{\delta}{\delta x} (AUS) = \frac{\delta}{\delta x} (AE \frac{\delta S}{\delta x}) + qS_T \quad (3-16)$$

Dispersion is due to variations in salinity and velocity from their average values. In one-dimensional equations the mass transfer due to velocity distribution is combined with variations in velocity and salinity due to turbulence, and represented by the longitudinal dispersion coefficient. In tidal-average models, dispersion must also include transport by tidal advection. This tidal-average dispersion coefficient must be determined empirically for each situation and is good only for the conditions under which the coefficient was determined. The time saved by using a tidal-average model is offset by the difficulty in determining the dispersion coefficient. The importance of dispersion decreases as the description of velocity and salinity becomes more complete.

The dispersion coefficient in the fresh water portion of the estuary accounts for the longitudinal mixing due to turbulent diffusion and shear induced velocity distribution in the transverse and vertical directions. Taylor (1954) was the first to analyze longitudinal dispersion in turbulent flow in pipes. He showed that after an initial period the longitudinal dispersion follows the gradient transport formulation with a dispersion coefficient proportional to the amount of shear in the longitudinal velocity profile. The dispersion coefficient is several orders of magnitude larger than the turbulent diffusion coefficient in the longitudinal direction.

Taylor calculated that the dispersion coefficient for steady uniform flow in a straight pipe should be:

$$E = 10.1 a u_* \quad (3-17)$$

where  $E$  is the dispersion coefficient,  $a$  is the pipe radius and  $u_*$  is the shear velocity.

Elder (1959) applied Taylor's method to two-dimensional open channel flow to give:

$$E = 5.9 D u_* \quad (3-18)$$

in which  $D$  is the depth of flow.

Harleman (1966), by noting :  $u_* = \sqrt{\frac{f}{8}} U$  and using the Chezy coefficient,

$C_h = \sqrt{\frac{8g}{f}} \frac{1}{n} R^{2/3}$ , expressed the dispersion coefficient in terms of the mean velocity as:

$$E = 77 n U R^{5/6} \text{ (in foot/secs units)} \quad (3-19)$$

$$= 63.2 n U R^{5/6} \text{ (in MKS units)}$$

where  $n$  is Manning's friction coefficient,  $U$  is mean velocity and  $R$  is the hydraulic radius.

As seen from Equation (3-13) dispersion depends on velocity variations ( $u''$ ) throughout the cross-sectional area. Equation (3-19) for two-dimensional flow, considers only the velocity variations in the vertical direction. Natural flows are three-dimensional and Fischer (1966) has shown that the existence of transverse velocity variations may cause the dispersion coefficient to be as much as 1000 times greater than that given by Equation (3-19).

Fischer's (1967) analysis yielded the result:

$$E = 0.30 \frac{\overline{u''^2}}{u_*^2} \left( \frac{L}{R} \right)^2 R u_* \quad (3-20)$$

$$= 3.18 \frac{\overline{u''^2}}{u_*^2} \left( \frac{L}{R} \right)^2 n U R^{5/6}$$

where  $L$  is the distance on the water surface from the thread of maximum velocity to the most distant bank and  $\overline{u'^2}$  is the cross-sectional average of the squared velocity variations.

Taylor's analysis is limited to large times after introduction of a substance into the flow.  $T_c$ , a time scale for cross sectional mixing may be defined as:

$$T_c = \frac{\lambda^2}{e} \quad (3-21)$$

where  $\lambda$  is the distance over which diffusion must take place before the gradient transport formulation becomes applicable (e.g. the distance from the point of maximum velocity in the cross section to the channel boundary) and  $e$  is the turbulent diffusion coefficient in the corresponding direction.

In steady flow the dispersion coefficient reaches a constant value after an initial period on the order of  $T_c$ . In oscillating flow, if the period of oscillation is much longer than  $T_c$ , the substance will disperse at the same rate as if the flow were steady. If the period of oscillation is much shorter than  $T_c$ , no dispersion could take place, the substance would be carried back and forth across its initial position. Thus dispersion in oscillating flow depends on a dimensionless parameter:

$$T' = \frac{T}{T_c} \quad (3-22)$$

where  $T$  is the period of oscillation.

The dependence of the dispersion coefficient on  $T'$  has been found analytically for one case of simple geometry (Okubo 1967) and

numerically for more complicated geometries, (Holley et al., 1970). The results are displayed in Figure 3 of Holley et al (1970).

For flow in natural channels dispersion may result from velocity gradients in either the vertical or transverse directions. Two dimensionless time parameters can then be defined:

$$T'_t = \frac{T}{\frac{b^2}{e_t}} \quad (3-23)$$

$$T'_v = \frac{T}{\frac{D^2}{e_v}} \quad (3-24)$$

where  $T'_t$  is in the transverse direction,  $T'_v$  is in the vertical direction and  $b$  is the half width, the distance over which diffusion takes place. Elder (1959) found for a logarithmic velocity profile:

$$e_v = 0.067 Ru_* \quad (3-25)$$

For straight, wide channels,  $e_t$  has been found empirically. (Fischer 1969).

$$e_t = 0.23 Ru_* \quad (3-26)$$

The limiting value ( $E_\infty$ ) for large  $T'$  is the same as the dispersion coefficient for the steady flow corresponding to the average hydraulic conditons for the estuary flow. The limiting dispersion coefficient for the vertical direction may be approximated from (3-19):

$$E_{\infty v} = 63.2 n U R^{2/3} \quad (3-27)$$

The limiting dispersion coefficient for the transverse direction may approximated from Equation (3-20), assuming that  $D$  and  $R$  are essentially equal and  $L$  is the half-width  $b$ :

$$E_{\omega t} = 3.18 \frac{\overline{u'^2}}{u_*^2} \left( \frac{b}{R} \right)^2 \approx U R^{5/6} \quad (3-28)$$

For most estuaries:

$$T'_v \gg 1$$

$$T'_t \ll 0.1$$

therefore:

$$E_v = E_{\omega v} = 63.2 \approx U R^{5/6} \quad (3-29)$$

From Figure 3 of Holley et al (1970):

$$\frac{E_t}{E_{\omega}} = 10 (T')^2 \quad \text{for } T' \ll 1 \quad (3-30)$$

Therefore:

$$\begin{aligned} E_t &= 10 (T'_t)^2 E_{\omega t} \\ &= 1.68 \approx U R^{5/6} \left( \frac{T \overline{u'^2}}{b} \right)^2 \end{aligned} \quad (3-31)$$

Dividing (3-31) by (3-29) and introducing  $\frac{2}{\pi} U_T$ , the average tidal velocity during one half period where  $U_T$  is the amplitude of the tidal velocity. Gives:

$$\frac{E_t}{E_v} = 0.011 \left( \frac{U_T T}{b} \right)^2 \left[ \frac{\overline{u'^2}}{\left( \frac{2}{\pi} U_T \right)^2} \right] \quad (3-32)$$

The term in brackets ranges between 0.01 and 0.04 (Holley et al 1970).

Therefore:

$$\frac{E_t}{E_v} = TS \left( \frac{U_T T}{b} \right)^2 \quad (3-33)$$

where TS is a constant on the order  $10^{-4}$ .

Substituting (3-29) for  $E_v$ :

$$E_v + E_t = 63.2 \approx U R^{1/6} \left[ 1 + TS \left( \frac{U_T T}{b} \right)^2 \right] \quad (3-34)$$

Equation (3-34) is the dispersion coefficient in the fresh water portion of the estuary.

The more non-uniform the velocity distribution the larger the dispersion coefficient must be. Therefore, much larger dispersion coefficients are expected in the salinity intrusion region compared to those found in the non-saline tidal region. In the saline portion of a partially mixed estuary the dispersion coefficient is closely related to the gravitational circulation. Since the gravitational circulation depends on the salinity distribution it is clear that  $E_G$ , the dispersion coefficient for dispersion due to gravitational circulation, will depend on the salinity gradient.

An expression for  $E_G$  is derived in the appendix by integrating Hansen and Rattray's (1965) similarity solutions for gravitational circulation. (See Appendix for definitions of terms and symbols)

$$E_G = \frac{U_f^2 D^2}{K_v} \left[ \frac{2}{105} + \frac{19}{420} \left( \frac{\nu Ra}{48} \right) + \frac{19}{630} \left( \frac{\nu Ra}{48} \right)^2 \right] \quad (A-17)$$

From Hansen and Rattray's Figure 4 (1965),  $\frac{\nu Ra}{48}$  is of order 10 or larger for Virginia estuaries. Therefore the third term on the right in equation (A-17) dominates the other terms. Let:

$$E_G = \frac{19}{630} \left( \frac{1}{48} \right)^2 \frac{U_f^2 D^2}{K_v} (\nu Ra)^2 \quad (3-35)$$

By definition:

$$\nu Ra = \frac{g^2 k^2 D^2}{U_f^2 A_v} \left( \frac{\delta S}{\delta x} \right) \quad (3-36)$$

substituting equation (3-16) and

$$g = 9.8 \text{ m/sec}^2$$

$$k = 7.5 \times 10^{-4} \text{ 1/ppt}$$

the dispersion due to gravitational circulation may be written as:

$$\begin{aligned} E_G &= \frac{19}{630} \left( \frac{1}{48} \right)^2 \frac{g^2 k^2 D^2}{K_v A_v^2} \left( \frac{\delta S}{\delta x} \right)^2 \\ &= 7.1 \times 10^{-10} \frac{D^2}{K_v A_v} \left( \frac{\delta S}{\delta x} \right)^2 \end{aligned} \quad (3-37)$$

In stratified flow (Officer 1976):

$$K_v = K_o (1 + \beta Ri)^{-2} \quad (3-38)$$

$$A_v = A_o (1 + \beta Ri)^{-1} \quad (3-39)$$

where  $K_o$  and  $A_o$  are the values for homogeneous flow and  $Ri$  is a gradient Richardson number. The Richardson number,  $Ri$ , is a comparison of the stabilizing forces of density stratification to the destabilizing forces of velocity shear. It is expressed:

$$\begin{aligned} Ri &= \frac{g}{\rho} \frac{\delta \rho}{\delta z} / \left( \frac{\delta u}{\delta z} \right)^2 \\ &= gk \frac{\delta S}{\delta z} / \left( \frac{\delta u}{\delta z} \right)^2 \end{aligned} \quad (3-40)$$

Officer (1976) defines  $\beta = 1$ .

Substituting (3-38) and (3-39) into (3-37):

$$E_G = 7.1 \times 10^{-10} \frac{D^2}{K_o A_o^2} (1 + \beta Ri)^4 \left( \frac{\delta S}{\delta x} \right)^2 \quad (3-41)$$



In homogeneous flow

$$K_o \approx A_o \approx \gamma DU, \text{ where:} \quad (3-42)$$

$$\gamma = 0.067 \frac{U_*}{\bar{U}} \quad (\text{Fischer et al 1979}) \quad (3-43)$$

In most coastal plain estuaries:

$$\gamma \approx 3 \times 10^{-4} \quad (\text{Pritchard 1960}) \quad (3-44)$$

Therefore:

$$E_G \approx 27 \frac{D^3}{\bar{U}^3} (1 + \beta Ri)^4 \left( \frac{\delta S}{\delta x} \right)^2 \quad (3-45)$$

In the Rappahannock:

$$D \approx 6 \text{ m}$$

$$U \approx 0.25 \text{ m/sec}$$

After substitution:

$$E_G = \alpha_1 (1 + \beta Ri)^4 \left( \frac{\delta S}{\delta x} \right)^2 \quad (3-46)$$

where  $\alpha_1$  is a constant on the order of  $10^7$  when  $x$  is in meters and on the order of 10 when  $x$  is in kilometers.

To obtain an expression for  $Ri$ , equation (A-9) for  $\frac{S}{S_o}$  is evaluated at the surface where  $\frac{Z}{z} = 0$  to give:

$$\frac{S_s}{S_o} = 1 + \frac{\nu}{M} - \frac{7}{120} + \frac{\nu Ra}{48} \left( -\frac{1}{12} \right) \quad (3-47)$$

Equation (A-9) is evaluated at the bottom where  $\frac{Z}{z} = 1$  to give:

$$\frac{S_b}{S_o} = 1 + \nu \xi + \frac{\nu}{M} \left( \frac{1}{4} - \frac{1}{8} - \frac{7}{120} + \frac{\nu Ra}{48} \left( \frac{1}{2} - \frac{3}{4} + \frac{2}{5} - \frac{1}{12} \right) \right) \quad (3-48)$$

Subtracting (3-47) from (3-48) gives:

$$\frac{S_b - S_s}{S_o} = \frac{\nu}{M} \left[ \frac{1}{8} + \frac{1}{320} \nu Ra \right] \quad (3-49)$$

The parameters  $\frac{M}{\nu}$  and  $\nu Ra$  are not easily measurable because they contain the turbulent viscosity and diffusion coefficients, but they depend on the bulk parameters of river flow, tides, and cross-sectional area. Hansen and Rattray (1966) found the relationships

$$\frac{M}{\nu} = 0.05 P^{-1/2} \quad (3-50)$$

Where:

$$P = \frac{U_f}{\bar{U}_t} \quad \text{the ratio of fresh water inflow per unit area of cross}$$

section to the root mean square tidal current speed.

$$\nu Ra = 16 F_m^{-1/4} \quad \text{where:} \quad (3-51)$$

$$F_m = \frac{U_f}{U_d}, \quad \text{the densimetric Froude number.}$$

$$U_d = \sqrt{g D \Delta \rho / \rho} \quad \text{the densimetric velocity.}$$

$\Delta \rho$  = the density difference between fresh water and sea water.

Substituting into Equation (3-49) gives:

$$\frac{\delta S}{S_o} = 20 P^{1/2} \left( \frac{1}{8} + \frac{1}{20} F_m^{-1/4} \right) \quad (3-52)$$

In the Rappahannock the densimetric Froude number is approximately 0.011. Therefore :

$$\frac{1}{20} F_m^{-1/4} \approx 1.47 \quad \text{which is much greater than } \frac{1}{8} .$$

Equation (3-52) becomes:

$$\begin{aligned}
 \delta S &= P^{1/2} F_m^{-1/4} S_o & (3-53) \\
 &= \left( \frac{U_f}{U_t} \right)^{1/2} \left( \frac{U_f}{\sqrt{gD\Delta\rho/\rho}} \right)^{-1/4} S_o \\
 &= \left( \frac{U_f}{U_t} \right)^{1/2} \left( \frac{U_f}{U_t} \right)^{-1/4} \left( \frac{U_t}{\sqrt{gD\Delta\rho/\rho}} \right)^{-1/4} S_o \\
 &= \left( \frac{U_f}{U_t} \right)^{11/8} \left( \frac{U_t}{\sqrt{gD\Delta\rho/\rho}} \right)^{-1/4} S_o
 \end{aligned}$$

In the Rappahannock:

$$U_t \approx 0.25 \text{ m/sec}$$

$$\sqrt{gD\Delta\rho/\rho} \approx 1$$

Using these values:

$$\delta S = 2.8 \left( \frac{U_f}{U_t} \right)^{11/8} S_o \quad (3-54)$$

$$\frac{\delta S}{\delta z} = \frac{3}{D} \left( \frac{U_f}{U_t} \right)^{.65} \quad (3-55)$$

where  $S = S_o$ , the mean salinity of the cross-section

For vertical shear,  $\frac{\delta u}{\delta z} \approx \frac{U}{D}$ , Pritchard (1960) gave:

$$\begin{aligned}
 \frac{\delta u}{\delta z} &\approx .7 \left( \frac{U}{D} \right) \\
 &\approx .7 \left( \frac{0.25}{6} \right)
 \end{aligned}$$

Therefore:

$$Ri \approx \frac{9.8 \times 7.5 \times 10^{-4} \times \frac{3}{6} \times S \times \left( \frac{U_f}{U_t} \right)^{.65}}{\left( .7 \times \frac{0.25}{6} \right)^2}$$

$$Ri = a_2 S \left( \frac{U_f}{U_t} \right)^{.65} \quad (3-56)$$

After substitution:

$$E_G = a_1 \left[ 1 + a_2 S \left( \frac{U_f}{U_t} \right)^{.65} \right]^4 \left( \frac{\delta S}{\delta x} \right)^2 \quad (3-57)$$

Where  $a_1 \approx 10$

$$a_2 \approx 4$$

Equation (3-37) is normalized to the tidal flow at the mouth ( $Q_t$ ) and becomes

$$E_G = a_1 \left[ 1 + a_2 S \left( \frac{Q_f}{Q_t} \right)^{.65} \right]^4 \left( \frac{\delta S}{\delta x} \right)^2 \quad (3-58)$$

The expression for total dispersion coefficient becomes

$$E = 63.2 \pi U R^{1/6} \left[ 1 + TS \left( \frac{UT}{b} \right)^2 \right] + a_1 \left[ 1 + a_2 S \left( \frac{Q_f}{Q_t} \right)^{.65} \right]^4 \left( \frac{\delta S}{\delta x} \right)^2 \quad (3-59)$$

#### **D. Method of Solution**

The governing partial differential equations are not generally solvable by analytical methods. The equations are solved by dividing the estuary into a series of finite segments. A system of finite-difference approximations to the original equations is obtained by integrating the equations of continuity, momentum and salinity, over the length of each segment (Williams, 1983). Predictions of surface level, velocity, and salinity are made by solving the finite-difference equations on a digital computer. A semi-implicit solution scheme was used.

## **E. Boundary and Initial Conditions**

### **1.) Upstream boundary conditions**

The upstream boundary of the model is located at the limit of tidal influence.

#### **a.) Dynamic condition**

There are two methods for the specification of the upstream dynamic boundary conditions. One method is to treat the freshwater discharge as flow through the most upstream transect. This method is used when the river bottom has a continuous slope at the limit of the tide. In the second method the discharge through the most upstream transect is set to zero and the freshwater input is treated as lateral inflow into the most upstream reach. The freshwater flow does not contribute any momentum to the system in the second method. This method is used when there is a fall line at the limit of tidal influence.

#### **b.) Salinity condition**

The salinity intrusion in a large coastal plain estuary is always well downstream of the tidal limit. Therefore salinity at the upstream boundary is always taken as zero.

### **2.) Downstream boundary conditions**

The downstream boundary of the model is located at the river mouth.

#### **a.) Dynamic condition**

The water surface elevation at the mouth is specified as a boundary condition. The model allows two methods of supplying this input. One is to use hourly tidal heights as input. The model interpolates for the time steps between hours. The other is to use harmonic components to calculate the surface level at the mouth. The amplitude, phase and

speed of up to nine constituents are used in the calculation. The constituents used in this study, include lunar semidiurnal (M2), solar semidiurnal (S2), lunar elliptic semidiurnal (N2), lunar-solar declinational diurnal (K1), lunar quarter-diurnal (M4), lunar declinational diurnal (O1), lunar monthly (MM), solar semi-annual (SSA), and solar annual (SA).

#### b.) Salinity condition

The salinity boundary condition at the mouth is more complicated than that at the head. The salinity at the mouth can not be constant because the fresh water must leave the estuary during the ebb tide and this will decrease the salinity at the boundary. The tidal cycle is divided into two parts according to the direction of flow at the estuary mouth and a different boundary condition is applied for each part.

A bay salinity,  $S_0$ , is assumed to exist off the mouth of the estuary. During flood tide this bay water is advected into the estuary and at some stage of the tide, the salinity at the downstream boundary becomes equal to  $S_0$ .  $S_0$  can be specified as a function of time if bay salinity is known.

At the end of the ebb portion of the tidal cycle the salinity at the mouth is lower than the bay salinity. An adjustment period is allowed after the flow starts to flood and before the salinity at the mouth reaches that of the bay (Thatcher and Harleman 1972). In this model an input parameter is specified for the length of this adjustment period and the salinity is assumed to increase linearly during this period.

During ebb flow the salinity at the boundary is evaluated assuming the salt flux across the boundary is by advection only. The expression for the boundary salinity during ebb tide becomes:

$$S_{MU}^2 = S_{MU}^1 - (S_{MU}^1 - S_{MU-1}^1) \times \frac{U \Delta t}{\Delta x}$$

Where S is salinity, the superscript 1 refers to the value at the previous time step, the superscript 2 refers to the present time step. The subscript MU refers to the value at the downstream boundary, and the subscript MU-1 refers to the segment just upstream of the mouth. U is the velocity at the mouth,  $\Delta x$  and  $\Delta t$  are the distance and time steps used in the solution.

### 3.) Initial conditions

#### a.) Dynamic condition

The necessary initial conditions are the specification of surface elevation and discharge for each model reach at time equal to zero. At the start of the calculations the parameters are set to zero everywhere and the model is run for several tidal cycles to allow the parameters to converge to the values corresponding to a state of dynamic equilibrium.

#### b.) Salinity condition

The model requires that initial salinity conditions for each reach be read in at time = 0. It is assumed that the user has a rough approximation of the initial salinity distribution. The choice of initial conditions is somewhat arbitrary, after twenty cycles the salinities will converge to their equilibrium values.



## F. Comparison of Model with Analytical Solution

A numerical approximation to a differential equation or set of equations should be proved to provide a stable, convergent solution. A stable solution is one which does not oscillate or grow wildly. A convergent solution agrees with the solution of the original differential equation.

The numerical solution is tested empirically by comparison with a known, analytical solution. Stability is confirmed by conducting the numerical integration until a quasi-steady solution is achieved.

The model predictions of tidal range are tested against the solution to the one-dimensional, linearized equations of continuity and momentum applied to a frictionless, rectangular channel which is closed at one end and connected to the open sea at the other end.

These equations are:

$$\frac{\delta \eta}{\delta x} = -h \frac{\delta u}{\delta x} \quad (3-60)$$

$$\frac{\delta u}{\delta t} = -g \frac{\delta \eta}{\delta x} \quad (3-61)$$

The solution to the above equations for surface level as a function of location and time is given by Ippen (1966) as:

$$\eta = 2a \cos(\sigma t) \cos(kx) \quad (3-62)$$

Where:

$\eta$  = surface level,

$2a$  = tidal amplitude at closed end of the channel,

$\sigma = \frac{2\pi}{T}$ ,  $T$  = tidal period,

$k = \frac{2\pi}{c_o T}$ , wave number,

$c_0 = \sqrt{gh}$ , the phase speed,

$h$  = channel depth,

$t$  = time,

$x$  = distance from the head of the channel.

An expression for tidal amplitude  $A$ , at any location on the channel normalized by the amplitude at the mouth  $A_0$ , may be derived from equation (3-62).

$$\frac{A}{A_0} = \left| \frac{\cos(kx)}{\cos(kl)} \right| \quad (3-63)$$

where  $l$  is the length of the channel.

Parameters for use in (3-62) and (3-63) were chosen to roughly correspond to the Rappahannock River.

These parameters are:

$T = 12.42$  hours       $l = 160$  km

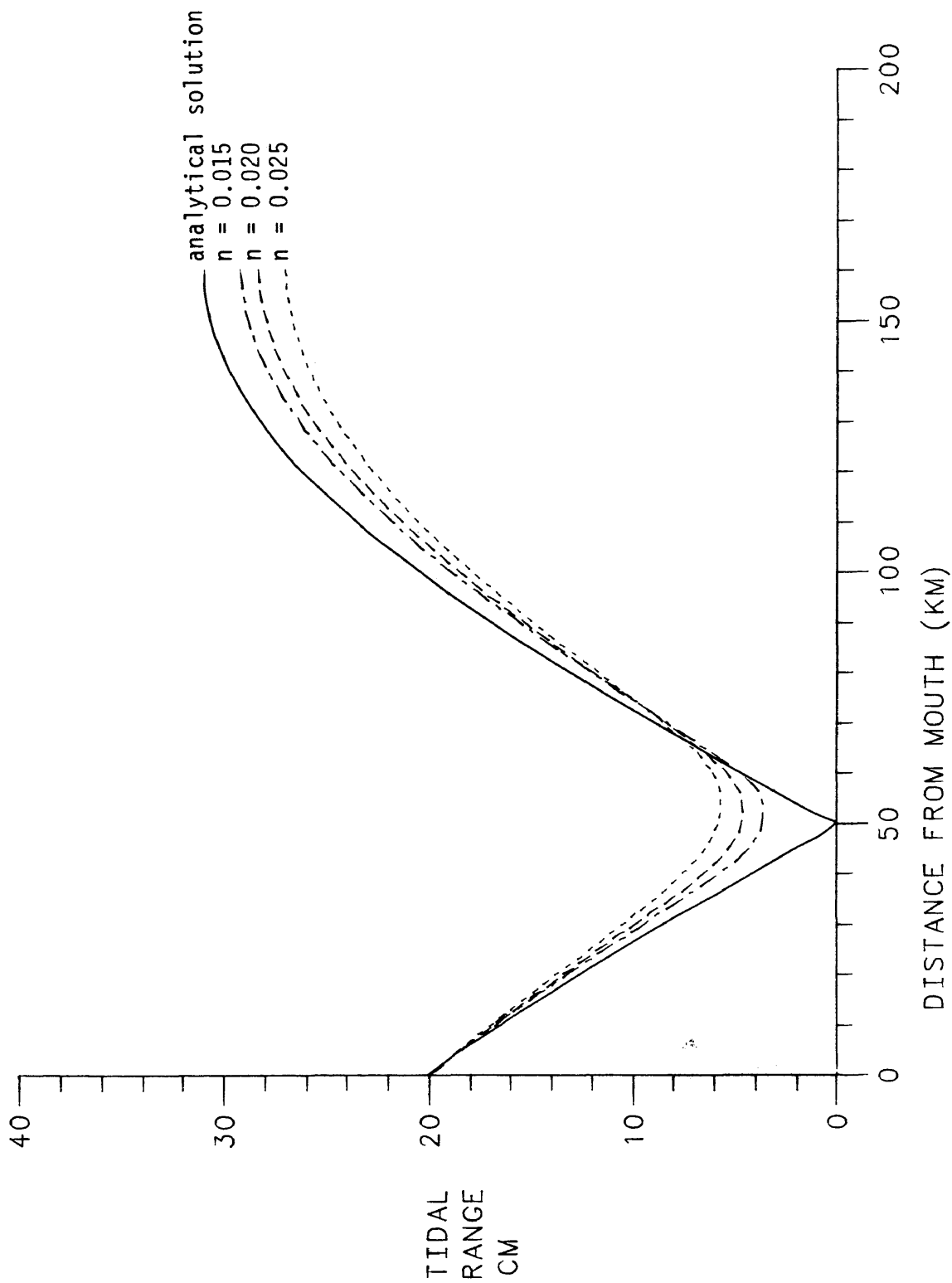
$h = 10$  meters       $A = 20$  cm

Salinity effects are not included in this test of tidal dynamics.

The model was first run with a Manning's  $n$  of 0.015. It was found that a time step of .02 tidal cycle (approximately 15 minutes) was optimal for the test run and was used for all the computational tests. A segment length of 4 km was used.

The model was run for 30 tidal cycles to establish the tidal regime with values of Manning's  $n$  progressively reduced from 0.025 to 0.015. The results, presented in Figure (3-1), show a convergence of the model solution as  $n$  is decreased. The model is not stable at  $n = 0.00$ . Since there is no analytical solution for the non-linear friction model, the numerical results can not be tested quantitatively.

Figure (3-1) shows a characteristic standing wave which results from superposition of two progressive waves traveling in opposite directions. The outgoing reflected wave is out of phase with respect to the incoming wave at a distance of a quarter wavelength from the head of the tide. This results in a nodal point of minimum tide range about 50 km from the mouth.



COMPARISON WITH ANALYTICAL SOLUTION

FIGURE 3-1

#### **IV. APPLICATION TO THE RAPPAHANNOCK RIVER**

##### **A. Model Set-Up**

The Rappahannock River rises on the eastern slope of the Blue Ridge Mountains and flows southeasterly to the Chesapeake Bay. It is approximately 176 km from the fall line at Fredricksburg to Windmill Point at the mouth.

Downstream of Tappahannock the river is broad and shallow, except for a central channel. Marshes line the river and its tributaries. At the mouth is a sill of approximately 10 m depth.

The Rappahannock is classified as a partially-mixed, coastal plain estuary. The dynamic interaction of tide, freshwater inflow and salinity determine the flow and salinity regimes.

The tide is primarily semi-diurnal. Due to the length of the Rappahannock the tidal wave is not a simple traveling or standing wave but exhibits characteristics of a mixture of the two. The tidal wave takes approximately nine hours to travel from the mouth to Fredricksburg, which is the limit of the tidal influence. The NOS Tide Tables show that the mean tide range increases from 37 cm at the mouth to 55 cm at Bowlers Rock. The range decreases at Leedstown to 46 cm and increases again to 85 cm at Fredricksburg. The spring tide ranges are 25% greater. The mean measured tidal current ranges from 30 cm/sec at

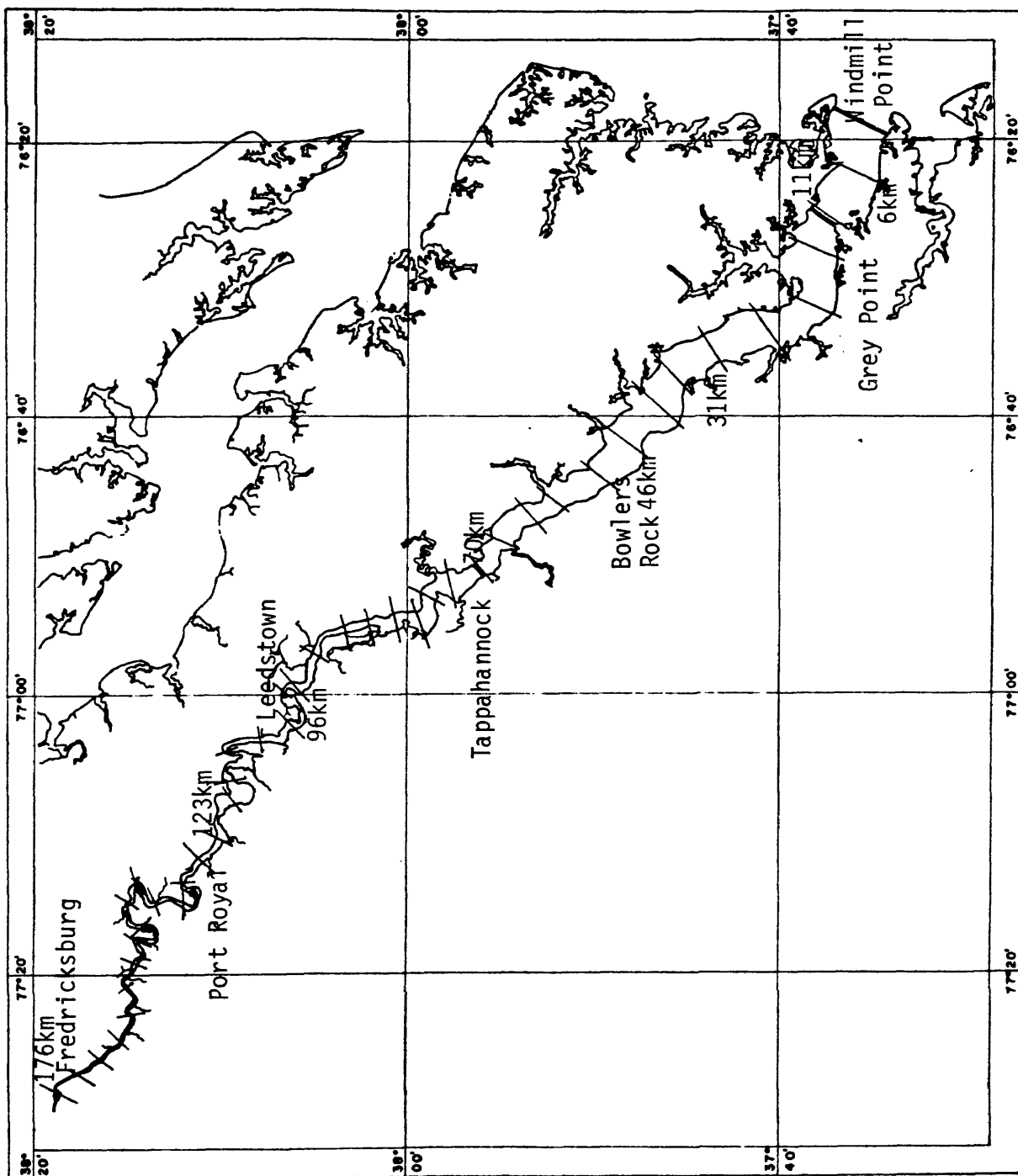
the mouth to a maximum of 67 cm/sec at Tappahannock and decreases to 37 cm/sec at Port Royal. The time between maximum ebb and low water is 1.5 hours at the mouth. At Port Royal, maximum ebb occurs more than 2 hours before low water.

The longitudinal salinity gradient is the forcing function for gravitational circulation. There is seasonal variation in the intrusion length in response to changes in freshwater inflow. The length of the intrusion varies from 60 to 100 km. The limit of the salinity intrusion is generally around Tappahannock, about 80 km from the mouth. The estuary is generally moderately stratified. Vertical salinity distribution responds to the seasonal variation in freshwater inflow and to the spring-neap tidal cycle. The vertical mean salinity at the mouth varies from 12 to 20 ppt. Its value is generally around 16 ppt. The salinity at the mouth is frequently found to be lower than that just upstream. A possible mechanism to explain this phenomena was explored by Hayward, Welch and Haas (1982).

The freshwater inflow is measured at Fredricksburg, where the river drains an area of  $4184 \text{ km}^2$ . The Rappahannock has experienced a wide range of inflow. The maximum flow of  $3964 \text{ m}^3/\text{sec}$  occurred on October 16, 1942. The minimum flow of  $0.14 \text{ m}^3/\text{sec}$  occurred on October 11, 1930. The yearly mean flow is  $45 \text{ m}^3/\text{sec}$ .

The estuary was divided into 44 unequal segments by locating 45 transects from the fall line to the mouth. Transects were located where bottom profiles were available and where the geometry of the cross-section was relatively simple and representative of that reach of the river. Figure (4-1) shows the locations of the transects. Each

transect is numbered starting at the upstream end with #1 reserved as an artificial transect for model calculations. The transect distance is measured from the mouth. Each transect has a surface width, cross-sectional area, and depth of center of moment. The depth of the centroid is taken as half the average depth of the transect. Segment  $i$  is defined as the volume between transect  $i$  and transect  $i+1$ . Each segment has a volume and surface area. The drainage area at  $i$  is the drainage area between transects  $i-1$  and  $i$ . It contributes to the segment  $i-1$ . The drainage area at 2 is the total drainage area upstream of segment 2. The Army Corps of Engineers conducted a bathymetric survey in 1973. The bottom profile data they obtained were used to determine cross-sectional areas by planimetry. Channel widths and segment lengths were determined from Coast and Geodetic Survey navigation charts. Drainage area values have been found for the Chesapeake Bay and its tributaries by Seitz (1971). The drainage area and geometrical data used in this study is presented in Table 1.



SEGMENTATION OF RIVER  
FIGURE 4-1



TABLE 1  
GEOMETRIC DATA

SEGMENT NUMBER	DISTANCE	SURFACE WIDTH	CROSS- SECTIONAL AREA	SURFACE AREA	VOLUME	DRAINAGE AREA	CENTER OF MOMENT
	KM	M	10**3 M**2	10**6 M**2	10**6 M**3	KM**2	M
2	176.51	91.44	.084	.310	.362	4184.42	0.46
3	173.61	126.52	.165	.308	.825	21.28	0.65
4	170.23	102.50	.310	.311	1.115	38.29	1.51
5	167.18	96.04	.282	.432	1.310	36.17	1.47
6	163.64	127.98	.442	.427	1.384	60.01	1.73
7	160.26	148.36	.416	.515	1.698	59.03	1.42
8	156.56	156.24	.435	.539	2.817	59.52	1.39
9	153.18	160.09	.434	.507	2.134	37.20	1.36
10	149.15	160.04	.571	.587	2.075	45.46	1.78
11	145.78	105.17	.783	.601	2.724	14.37	3.72
12	141.91	127.28	.646	.620	2.470	6.52	2.54
13	138.53	216.60	.789	.700	2.883	7.07	1.83
14	135.16	133.38	.885	.709	3.815	20.04	3.32
15	130.81	194.18	.837	1.660	3.961	24.23	2.18
16	126.79	267.54	1.051	2.300	4.739	59.52	2.10
17	123.09	160.94	1.186	4.884	5.484	67.31	3.78
18	119.87	327.56	1.498	3.621	7.244	46.60	2.29
19	116.33	172.34	1.544	3.922	8.488	36.24	4.48
20	112.15	287.06	1.582	1.140	8.223	38.83	2.88
21	107.80	401.12	1.895	2.040	8.370	49.19	2.36
22	103.94	570.95	2.330	3.450	10.480	51.78	2.10
23	99.44	223.62	2.117	2.030	9.294	31.07	4.75
24	95.57	413.46	2.783	3.240	12.965	7.77	3.46
25	91.23	807.06	2.903	2.850	12.512	18.12	1.80
26	86.89	483.00	2.691	2.590	10.376	25.89	2.94
27	83.51	655.21	2.895	6.670	13.796	23.30	2.29
28	79.65	1024.15	3.684	7.540	12.528	18.12	1.80
29	76.27	1176.53	3.730	3.300	11.599	62.13	1.58
30	73.85	1252.63	5.878	10.460	19.358	151.78	2.35
31	70.15	1895.29	5.141	8.090	21.868	147.57	1.36
32	66.13	2064.98	5.552	8.510	20.967	165.69	1.39
33	62.75	2330.93	6.678	12.380	37.112	139.80	1.43
34	58.25	3609.29	9.791	7.290	21.103	99.34	1.36
35	55.99	2819.79	8.692	17.400	55.762	95.79	1.58
36	50.84	4010.76	12.714	18.080	56.708	62.13	1.58
37	46.50	3599.22	13.384	23.610	74.545	144.01	1.86
38	41.67	4590.97	17.492	19.100	96.769	124.27	1.91
39	37.01	4519.81	23.971	20.680	142.848	124.27	2.65
40	31.38	4617.83	26.743	25.880	162.993	24.27	2.90
41	25.42	3587.77	27.343	18.330	124.010	82.84	3.90
42	20.92	2908.37	26.666	42.630	190.997	115.53	4.65
43	14.96	4126.57	35.306	15.080	140.960	19.09	4.50
44	11.26	3954.01	38.582	28.800	194.805	18.12	4.94
45	5.95	3290.93	33.167	28.850	174.012	20.71	5.21
46	1.13	5507.56	37.134	0.000	0.000	12.94	3.43

## B. Hydrodynamic Calibration

The model was first calibrated for mean tide range along the river. The fresh water inflow and surface level at the mouth are needed as forcing functions. The mean freshwater inflow in the Rappahannock is  $45 \text{ m}^3/\text{sec}$  at the head of the tide, this rate was used as a constant inflow for the model calibration. The input tidal height at the mouth is found from harmonic analysis. The function used is:

$$\eta = \sum_{n=1}^9 [ A_n \cos ( \sigma_n t + \phi_n ) ],$$

where  $A$  is the amplitude,  $\sigma$  is the phase speed, and  $\phi$  is the phase of each tidal constituent. The harmonic constituents of the tide were found by using the least-squares method of harmonic analysis (Kiley and Boon, 1978) on a twenty-nine day tide gauge record from Windmill Point at the mouth of the Rappahannock. The amplitude and phase of the six major constituents were found and employed in the model (Table 2). A time thirty cycles after model start up corresponded to a time of mean tide range.

The tidal range was calculated in the model by finding the difference in high and low water at each transect. The predicted range from the model was compared with the mean range from the NOS Tide Tables. The value of Manning's friction coefficient was varied until the model predicted range and the table predicted range agreed. Values for Manning's friction coefficient of 0.016 from the head to 37 km and 0.023 from there to the mouth were found to give good agreement with the tide tables. Near the mouth the estuary is broad and has shallow embayments which will increase the frictional resistance to flow. Therefore it is expected that the value of  $n$  will be greater near the

mouth than where the estuary is narrow and more nearly confined to a central channel. The model reproduces the mean range quite well (Figure 4-2). The standing wave characteristics are evident with the nodal point occurring near Leedstown, about 76 km from the head of the tide.

The times of the tide phases along the river are shown in Figures (4-3) and (4-4). For low tide the model simulates the phase speed quite well (Figure 4-4). The model predicts a greater speed for high tide than the tide tables do. This is particularly evident as the tide moves near the head of the river.

The times of maximum currents are shown in Figures (4-5) and (4-6). The phase speed of maximum flood current as it moves up river is predicted well by the model. The speed of maximum ebb is predicted well except at Port Royal, 127 km from the mouth, where the model predicts a greater speed of travel for the maximum ebb than the tables.

Figures (4-7) and (4-8) show the speed of slack before ebb and slack before flood as they move up river. Both are predicted well. The model's predicted speed of slack before ebb at Port Royal is less than that from the tables.

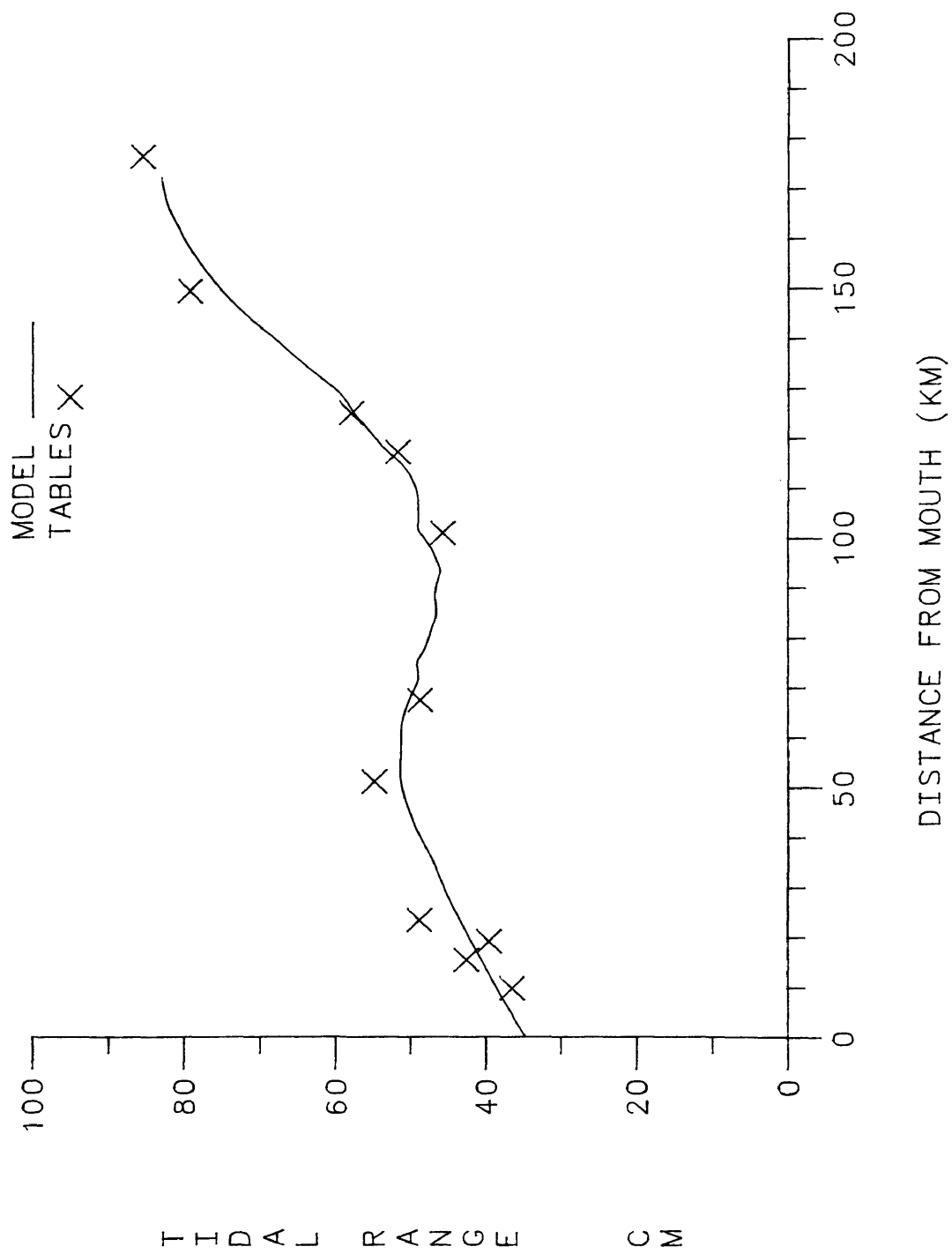
The model was then run for a time simulating the period from March 14 to October 30, 1973. An intensive survey was conducted on the lower Rappahannock during July 30 and 31 1973. This was during a period of spring tides. Current meters were deployed at varying depths along several transects. To compare the predicted currents with those measured during the intensive survey, the time varying fresh water inflow at the head and the surface level at the mouth were needed as boundary conditions. The fresh water inflow measured at the USGS gauging station at Fredricksburg was used as a daily input to the model.

The inflow for the time simulated is shown in Figure (4-9). During this period the inflow varied from 11 to 450 m<sup>3</sup>/sec. It was necessary to use predicted surface levels as boundary conditions at the mouth because a continuous tide record was not available for the entire time simulated. If tidal predictions are to be made for long periods of time, the simple cosine function using the harmonic constants is no longer adequate. Under these conditions it is necessary to use the harmonic model of the tide by Schureman (1958). This model uses the harmonic constants and the positions of the celestial bodies to generate predicted tides. These predicted tidal heights were used as inputs to the model. The predicted surface level at Windmill Point for the month of July 1973 is shown in Figure (4-10).

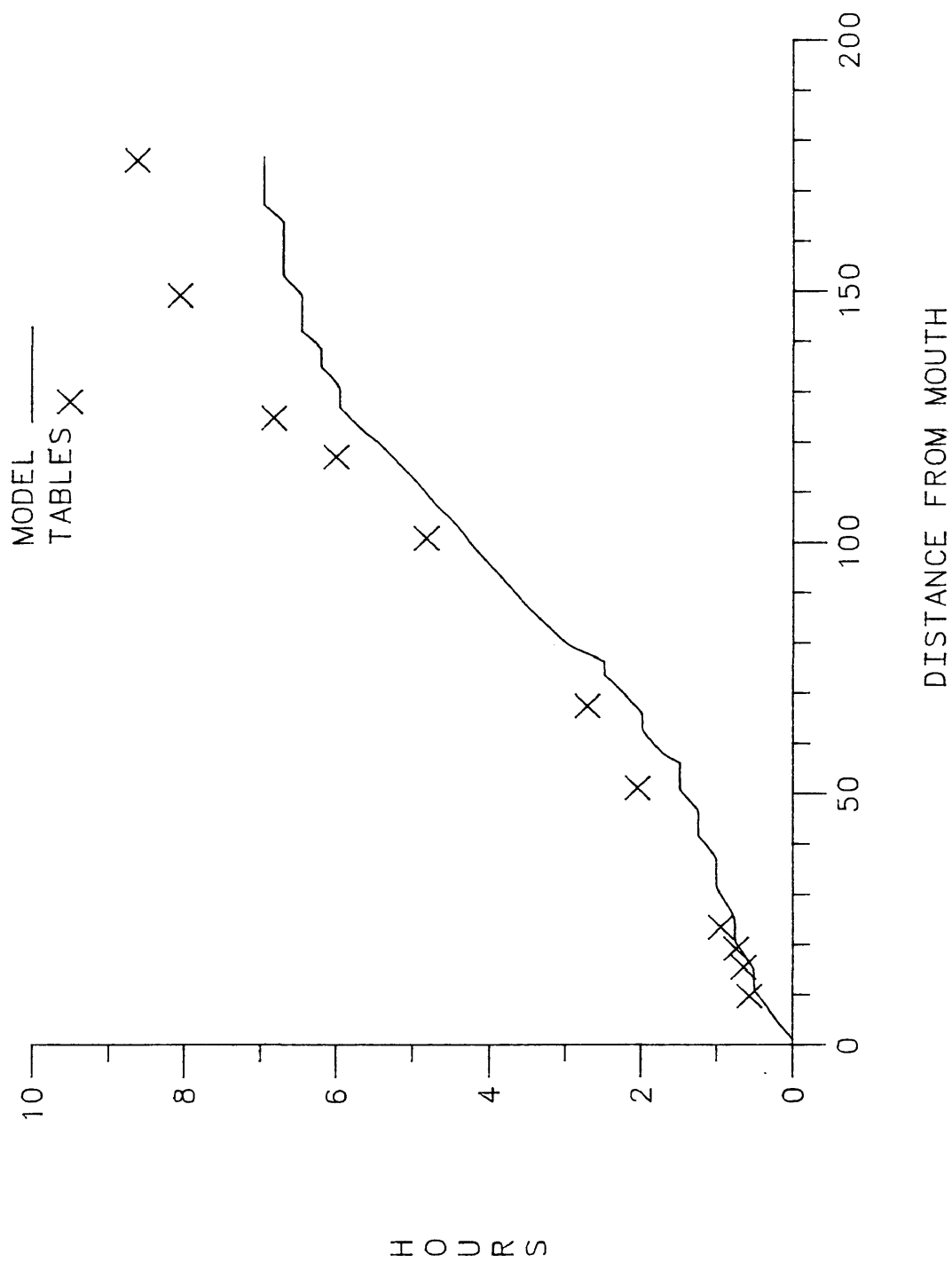
The measured current at Windmill Point was compared with the model output (Figure 4-11). The field data used for comparison is that from a meter at mid-depth in the channel. The predicted current is lower than that measured because the model predicts the cross-sectional mean velocity and the current meter was placed in the center channel where the current velocities are expected to be highest. The same is true at Grey Point as shown in Figure (4-12). The predicted current and measured current are in phase. The diurnal inequality is evident in both records.

**TABLE 2**  
**HARMONIC CONSTANTS**

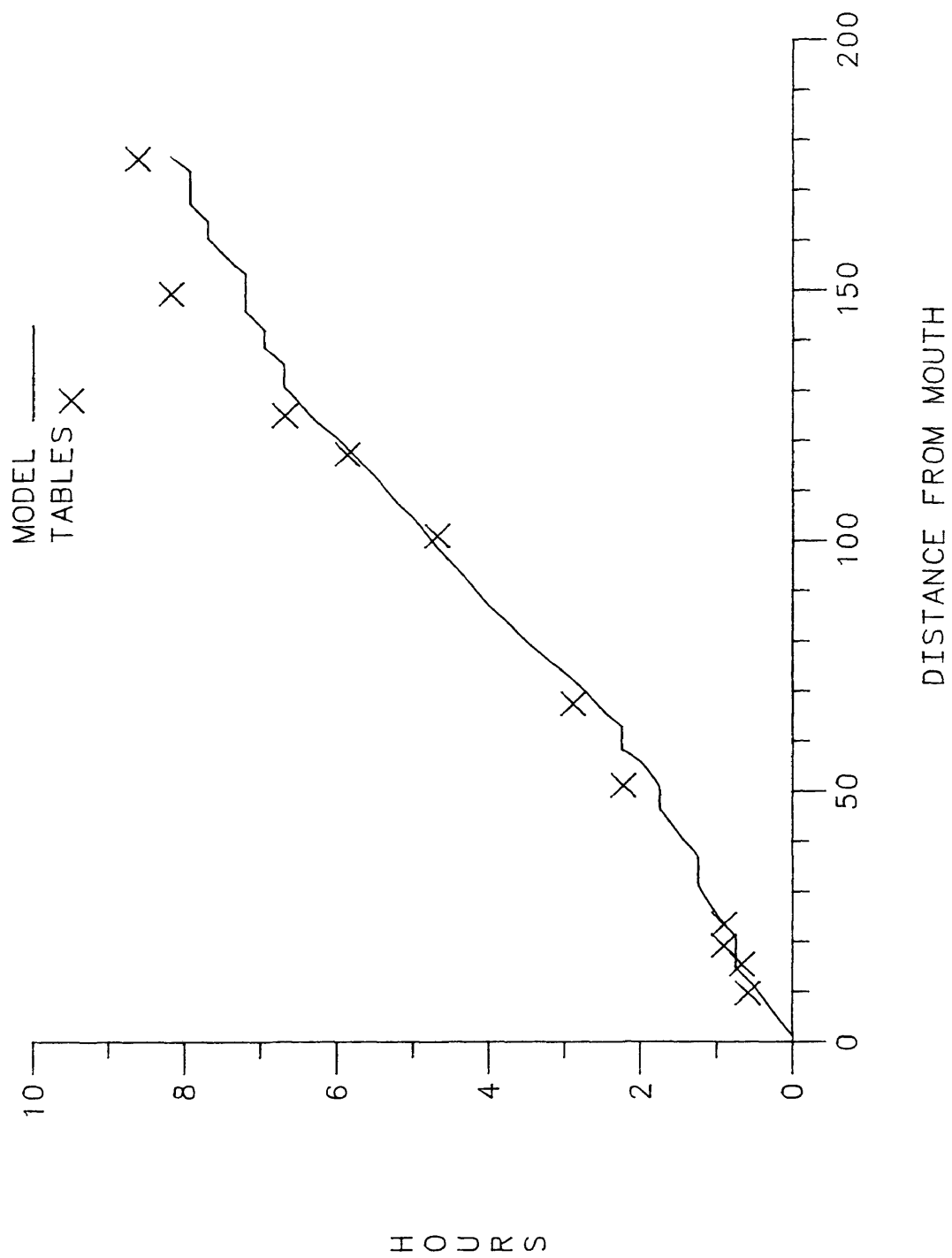
DESIGNATION	NAME	AMPLITUDE cm	PHASE radians	SPEED rad/day
M2	lunar semidiurnal	17.22	5.79	12.141
S2	solar semidiurnal	2.53	6.12	12.566
N2	lunar elliptic semidiurnal	3.63	5.39	11.913
K1	lunar-solar declinational dirunal	2.80	5.39	6.3
M4	lunar quarter-diurnal	0.88	3.26	24.282
O1	lunar declinational diurnal	2.35	0.22	5.84



MEAN TIDAL RANGE  
FIGURE 4-2

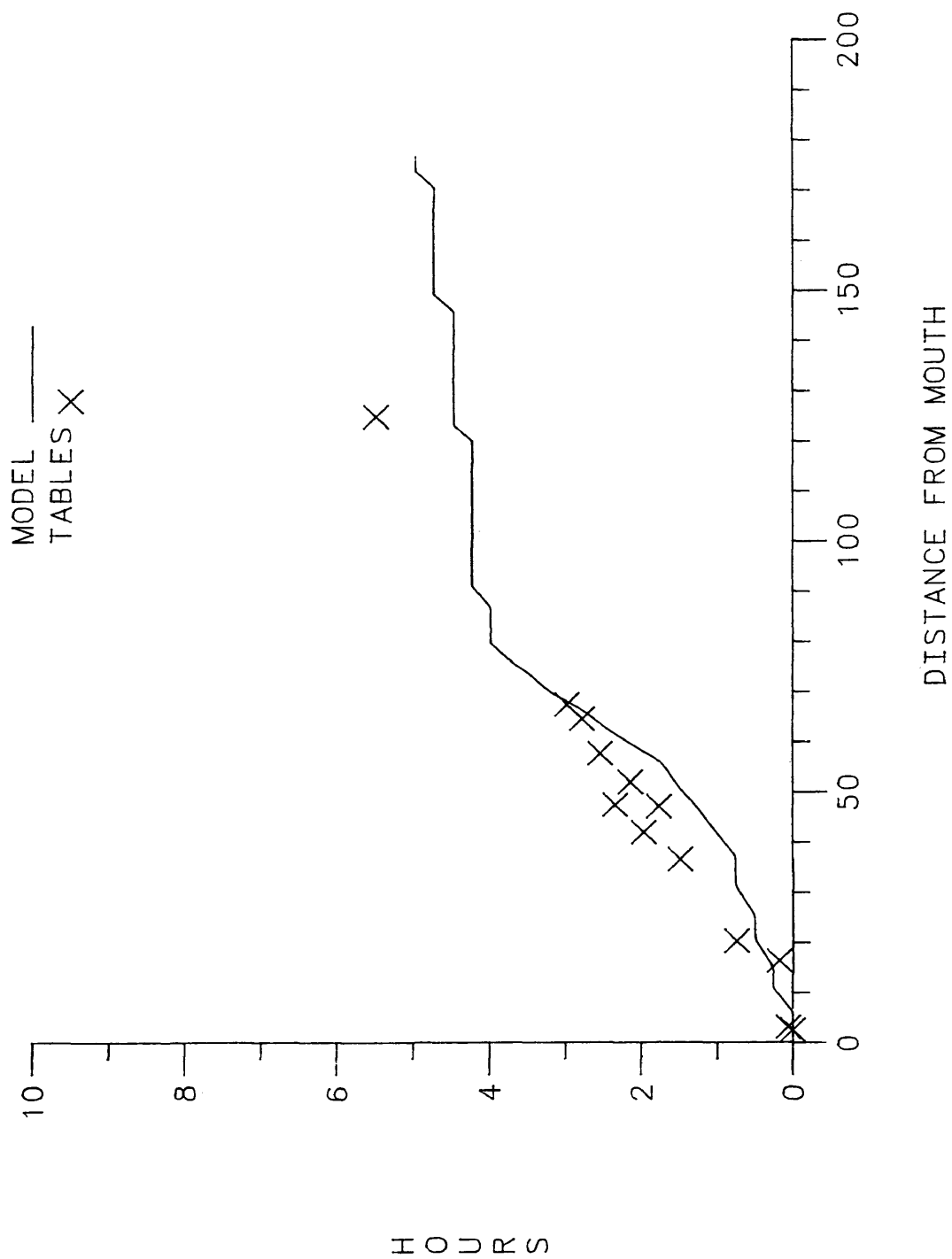


TIME OF HIGH TIDE  
FIGURE 4-3

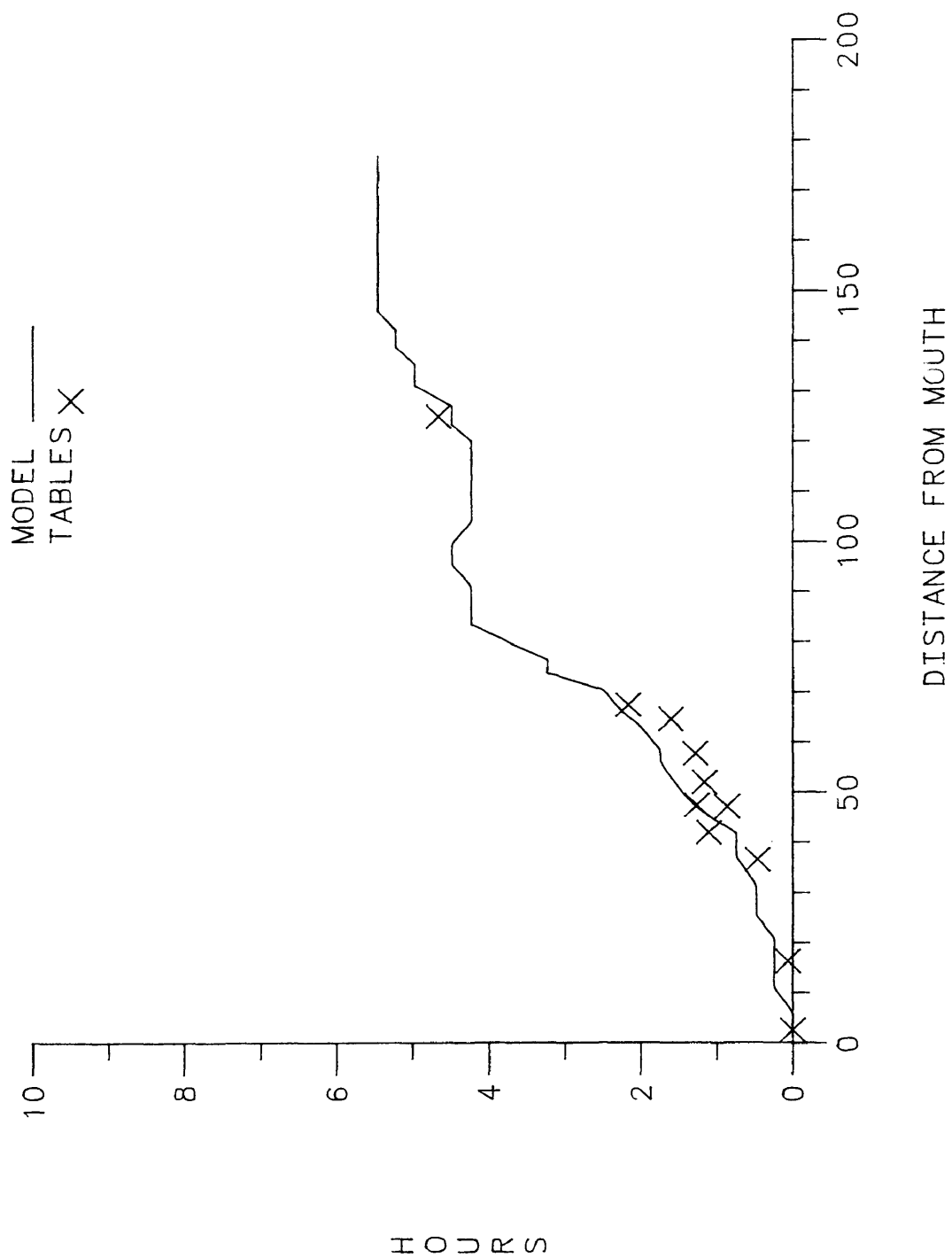


TIME OF LOW TIDE  
FIGURE 4-4

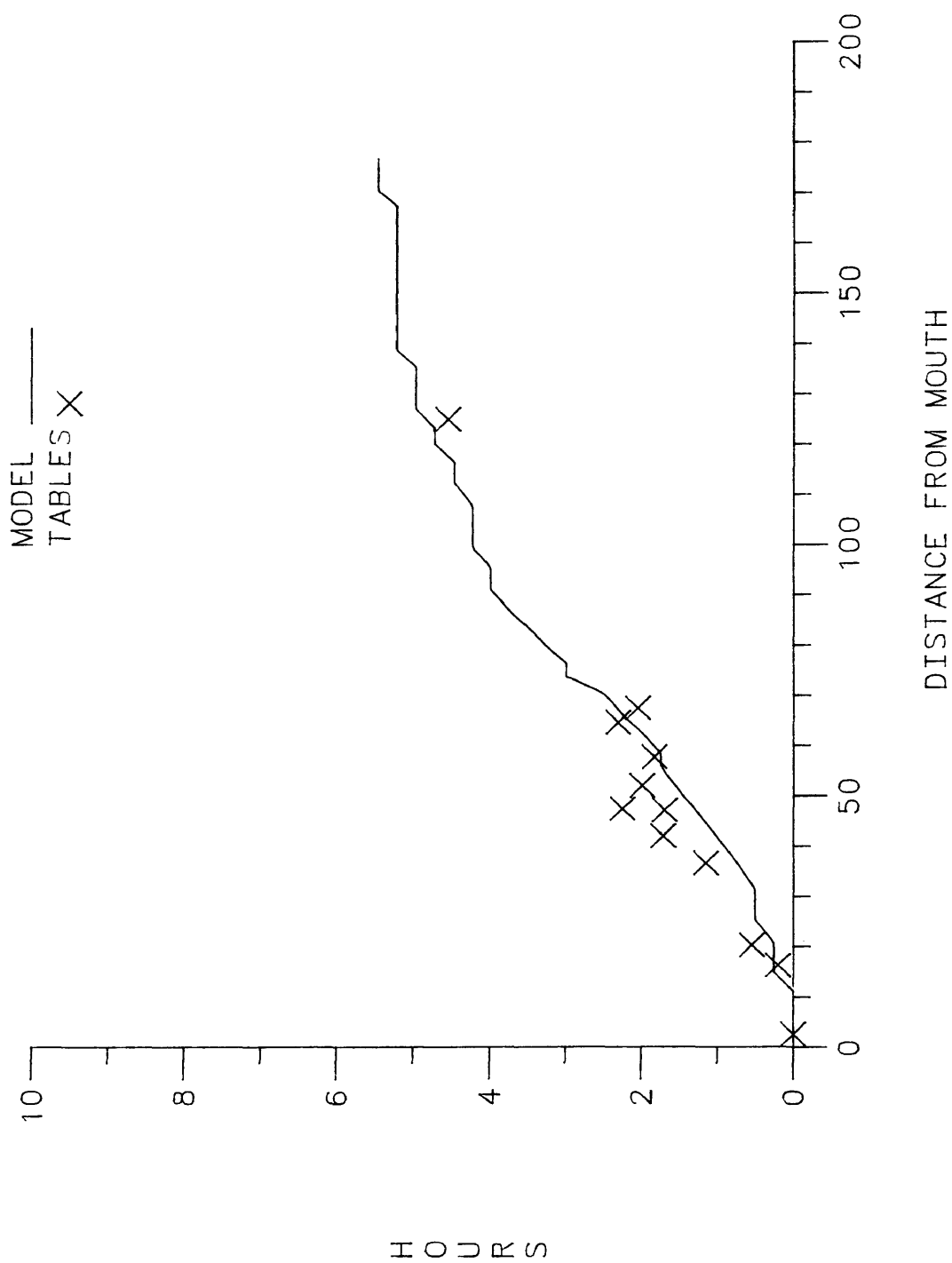




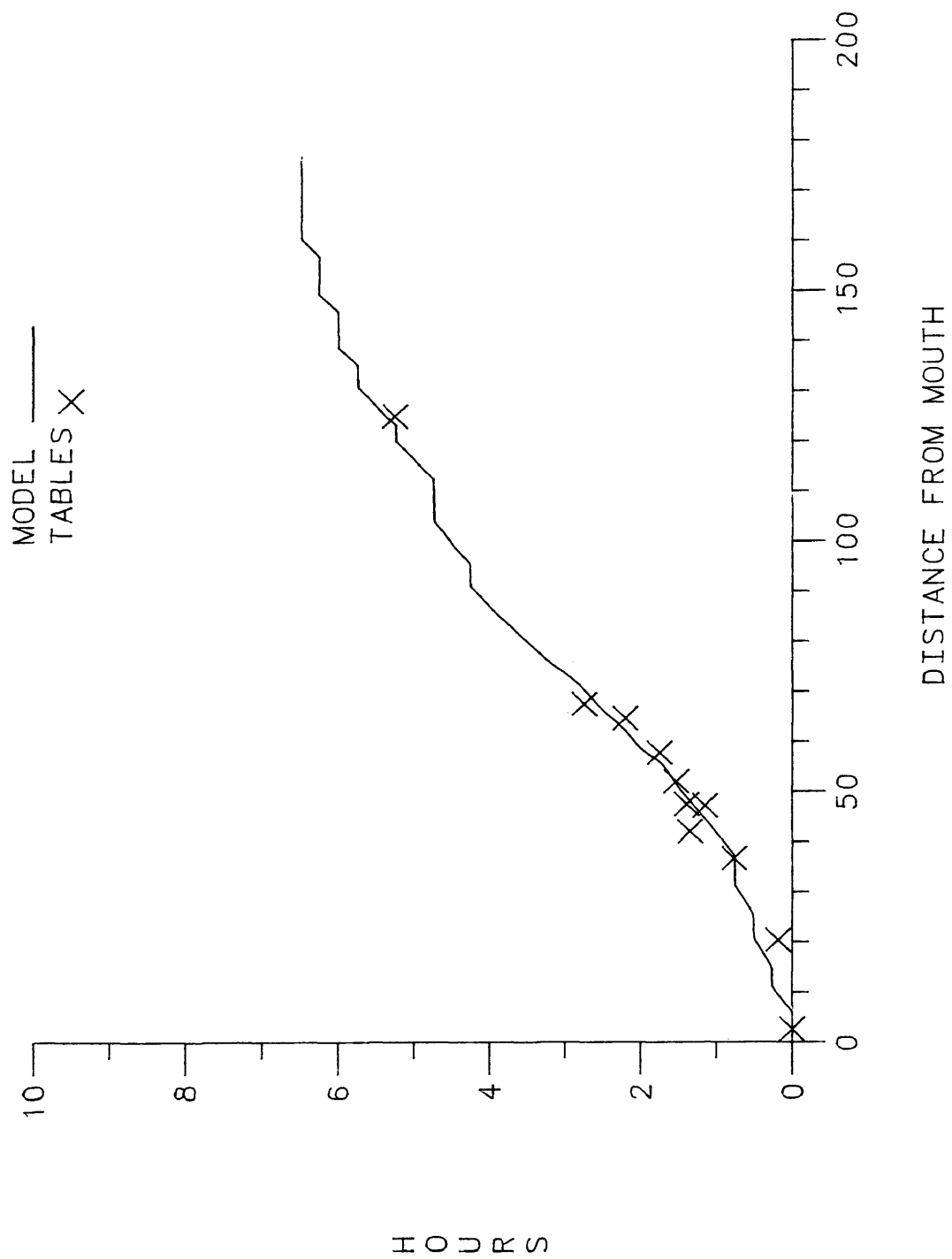
TIME OF MAXIMUM EBB  
FIGURE 4-5



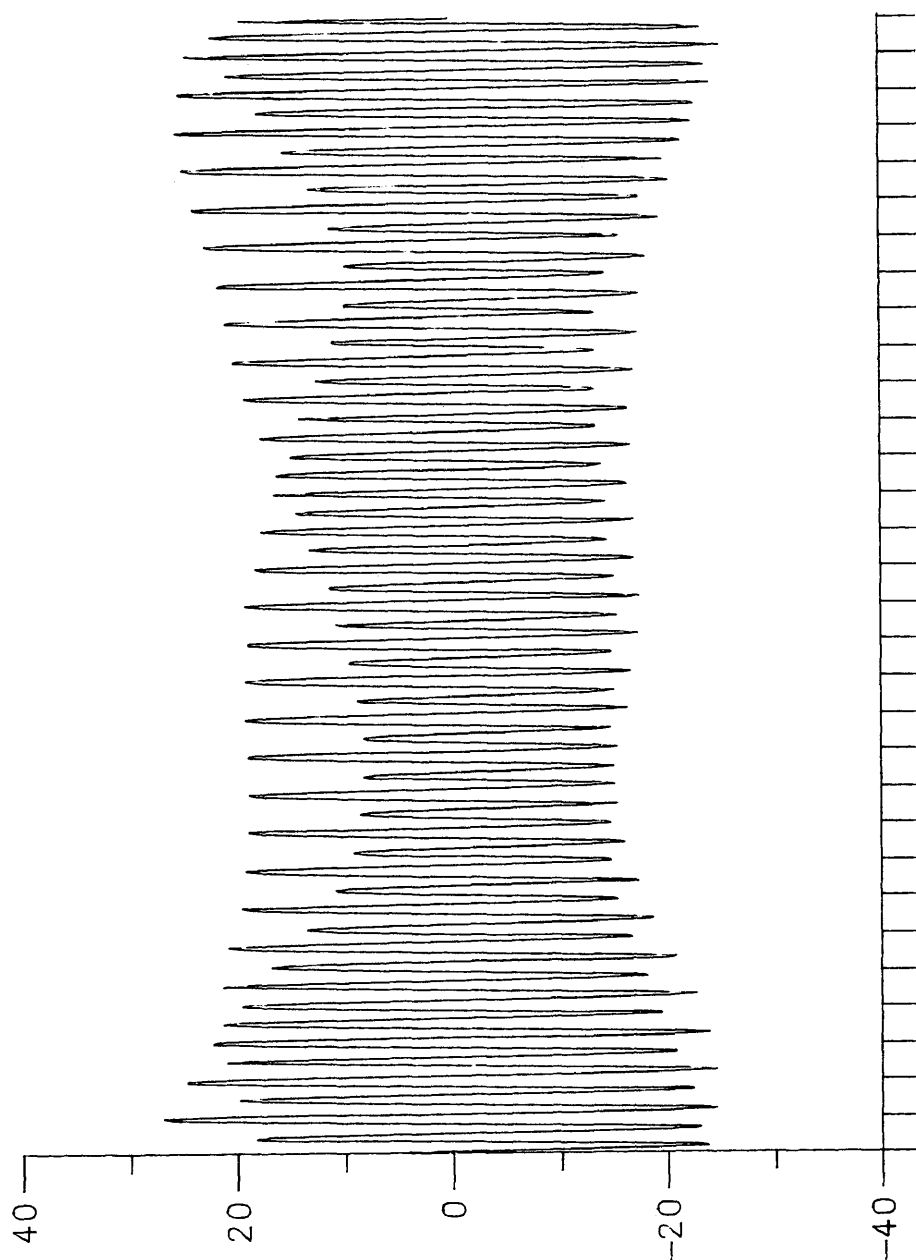
TIME OF MAXIMUM FLOOD  
FIGURE 4-6



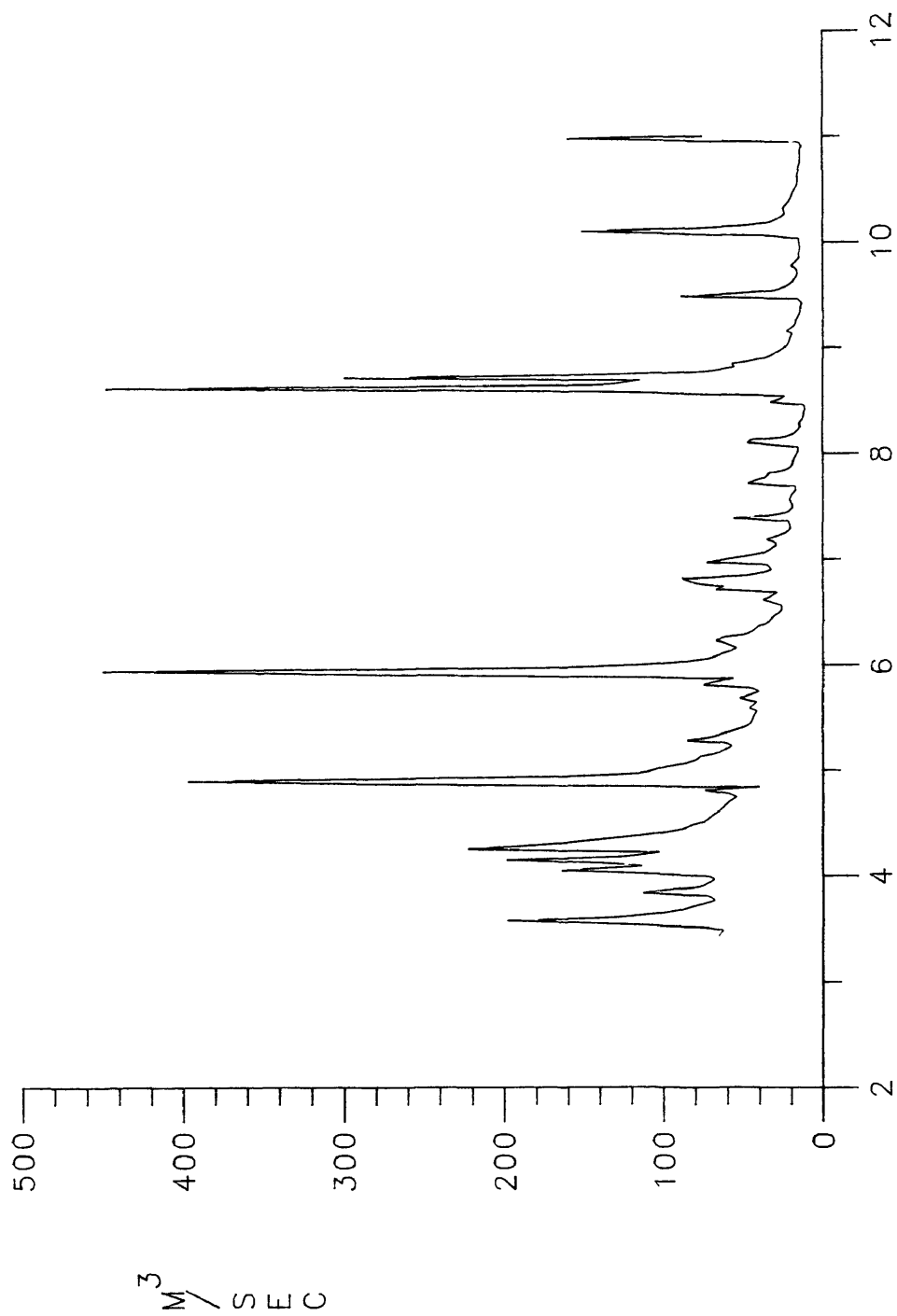
TIME OF SLACK BEFORE EBB  
FIGURE 4-7



TIME OF SLACK BEFORE FLOOD  
FIGURE 4-8



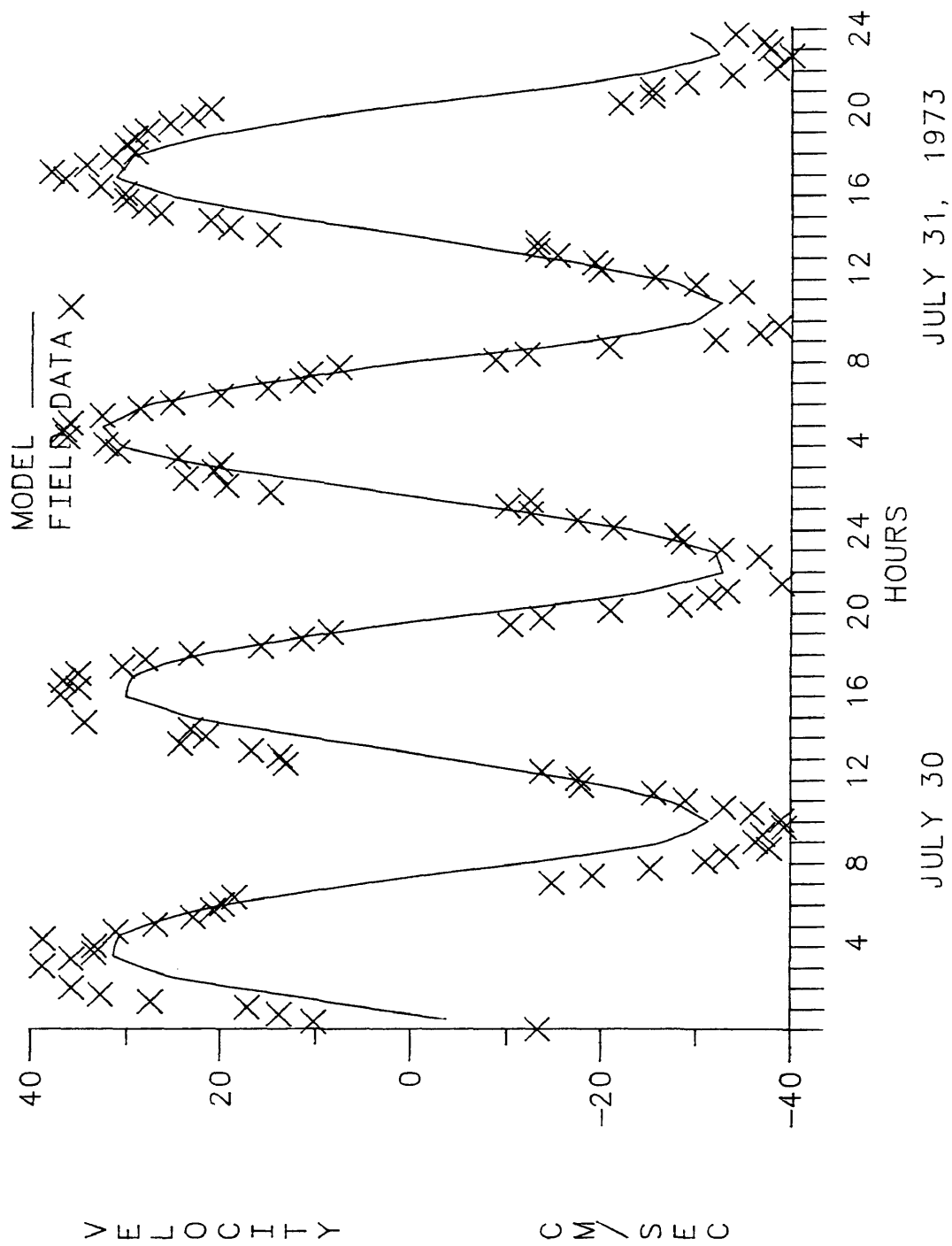
DAYS JULY 1973  
PREDICTED SURFACE LEVEL  
FIGURE 4-9



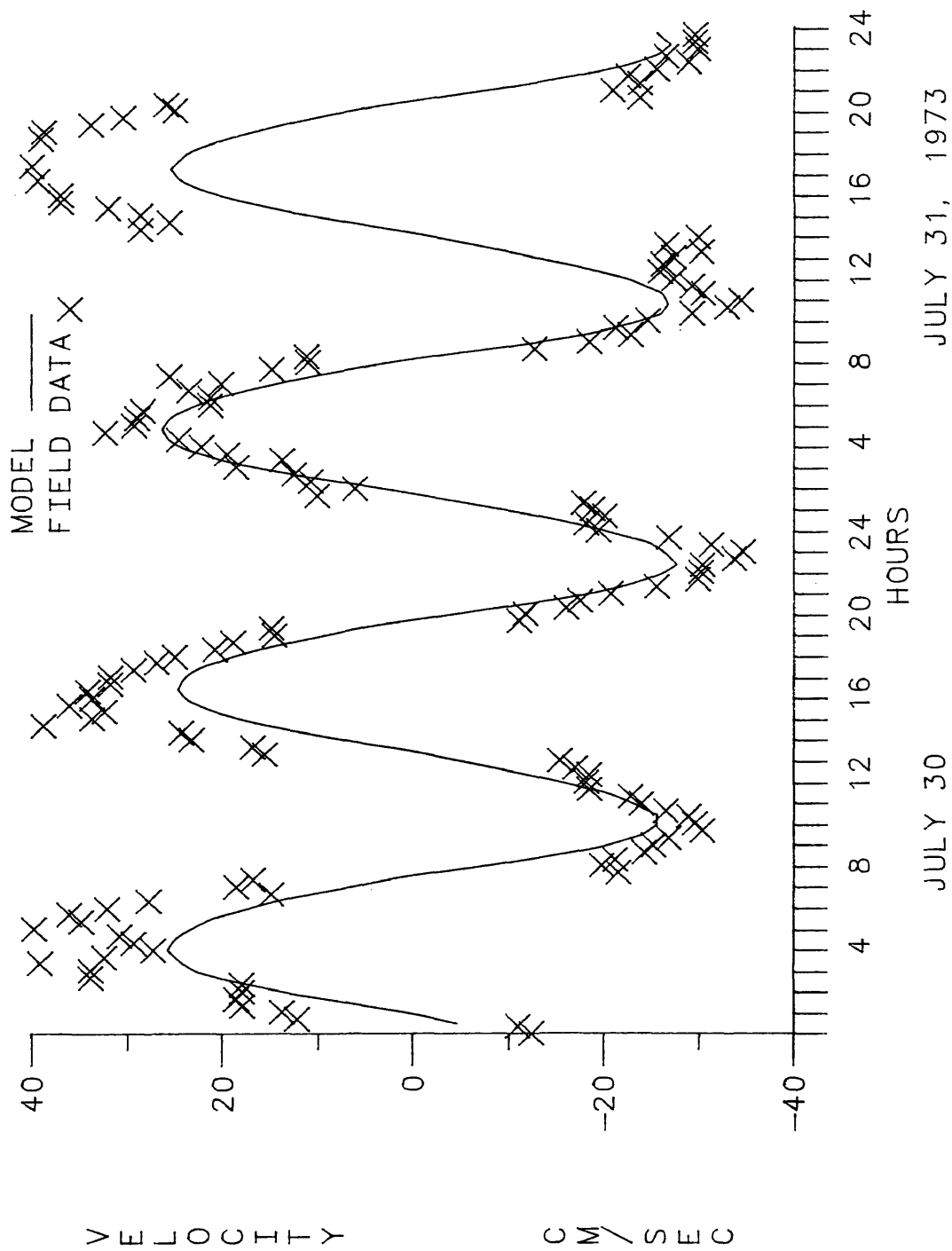
MONTH 1973

FRESHWATER INFLOW AT FREDRICKSBURG

FIGURE 4-10



CURRENT AT WINDMILL POINT  
FIGURE 4-11



CURRENT AT GREY POINT  
FIGURE 4-12



### C. Salinity Calibration

The model was calibrated for longitudinal salinity distribution using the data obtained on slack water surveys. Monthly surveys have been made from early spring through late fall since 1971. They have been conducted by following either slack before flood or slack before ebb as the tidal wave propagates upriver. At fixed stations temperature and conductivity were measured at two meter intervals from the surface to the bottom. The salinity values calculated from the temperature and conductivity measurements were averaged at each station to give a vertical mean salinity for that station. The model was again run for a time simulating the period from March 14 to October 30, 1973. The salinity data obtained on surveys during this period were used to calibrate the model for longitudinal salinity distribution.

Three boundary conditions are needed to run the model for the longitudinal salinity calibration. The daily fresh water inflow at the head and the surface level at the mouth were treated as they were in the hydrodynamic calibration of the tidal current for the same time period. In addition the vertical mean salinity at the mouth is needed as a boundary condition. The salinity at the mouth was input to the model daily. The values used were those obtained on slack water surveys when available and the values at dates between were interpolated. The boundary salinity varied from 13.5 to 18.5 ppt during the eight months. The slack surveys often found the salinity at the mouth to be lower than that found just upstream. When the slack survey indicated this condition the boundary salinity used in the model was extrapolated from the values upstream.

The value of salinity at slack water in the model was found for each segment by checking the discharge at each time step. When the discharge changed from positive to negative, that time step was considered to be the time of slack before flood. When the discharge changed from negative to positive that time step was considered to be the time of slack before ebb. The model considers the ebb direction as positive. The salinity values calculated by the model were compared with those measured on slack water surveys.

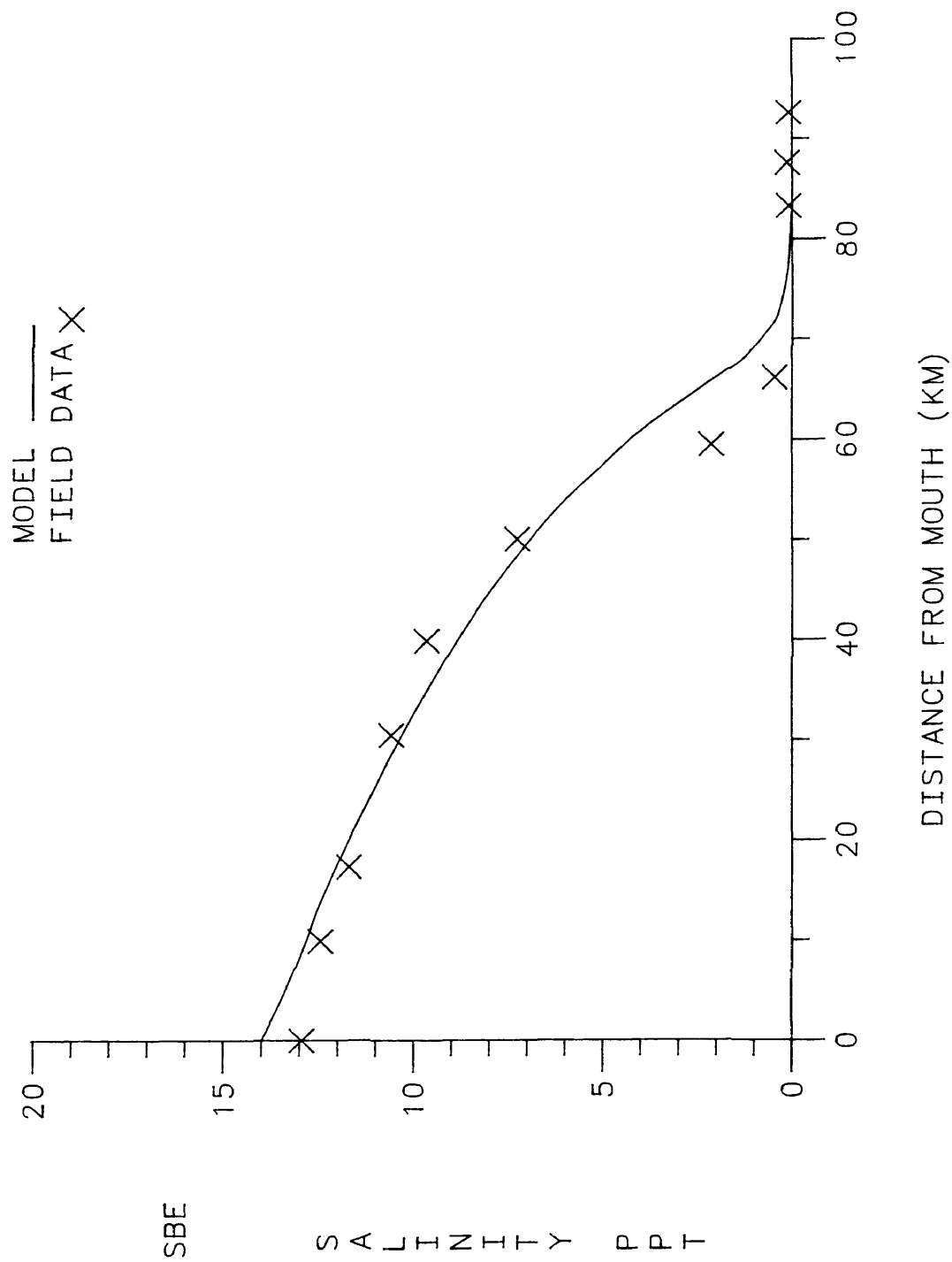
The model was run to determine the constants in the equation for dispersion due to gravitational circulation (Equation 3-58). The best fit was found to be for values of 10 and 5 for  $\alpha_1$  and  $\alpha_2$  in Equation (3-58). Equation (3-58) becomes:

$$E_G = 10.0 \left[ 1 + 5.0 \times S \times \left( \frac{Q_f}{Q_t} \right)^{.65} \right]^4 \left( \frac{\delta S}{\delta x} \right)^2 \quad (4-1)$$

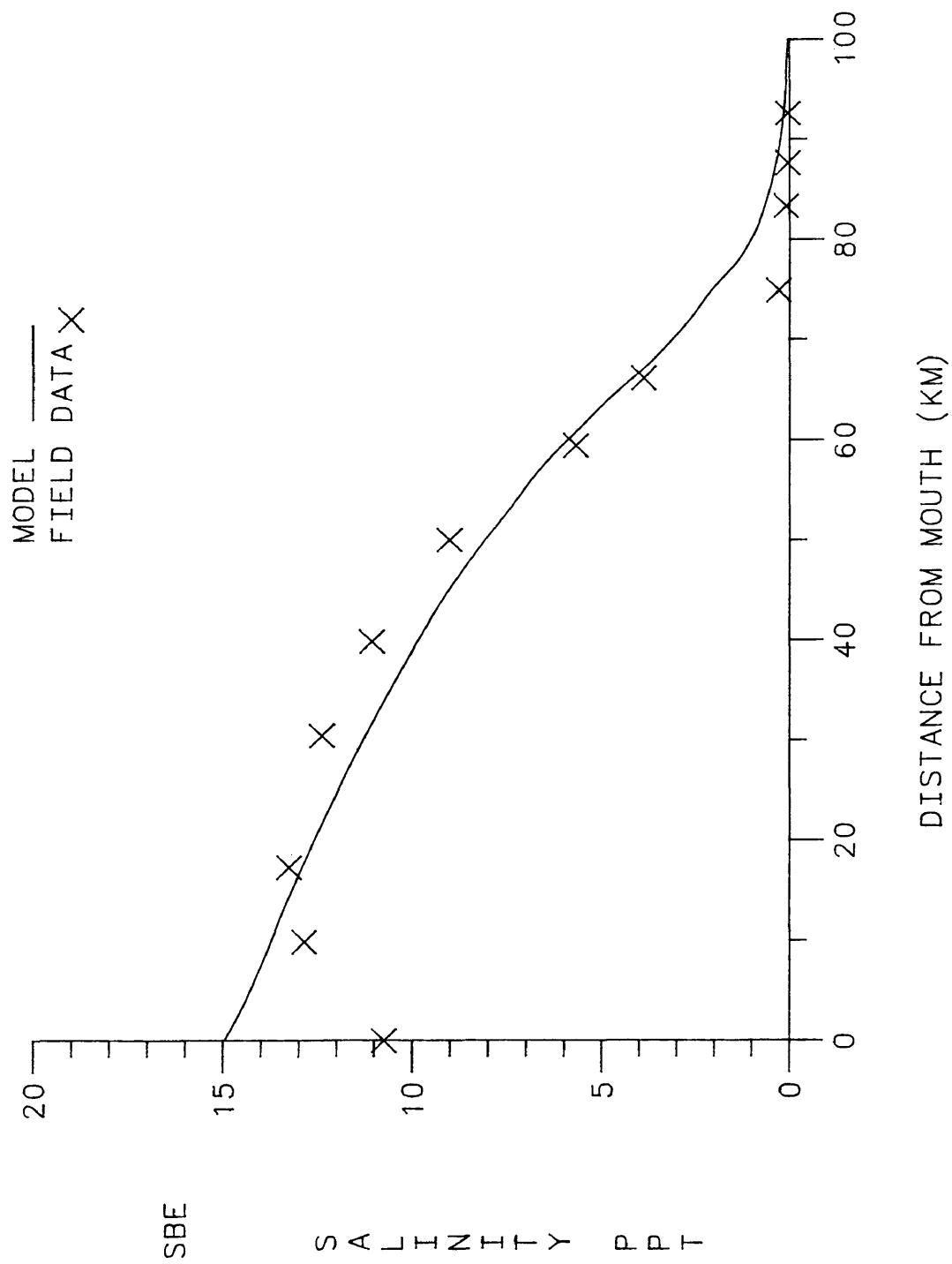
Figures (4-13) to (4-17) show the comparison of the longitudinal salinity distribution from the model and that from the slack water surveys. The length of the salinity intrusion is modeled well on all the dates. The model tends to under-estimate the salinity in the middle of the salinity region.

Salinity data from the intensive survey on July 30 and 31, 1973 was compared to the model predictions. During the intensive survey, transects were occupied in the lower Rappahannock. Temperature and conductivity measurements were made every hour, at two meter intervals from the surface to the bottom. The salinity values calculated from these measurements were averaged to give a vertical mean salinity for the transect. Due to the weather and equipment malfunctions, there are gaps in the data.

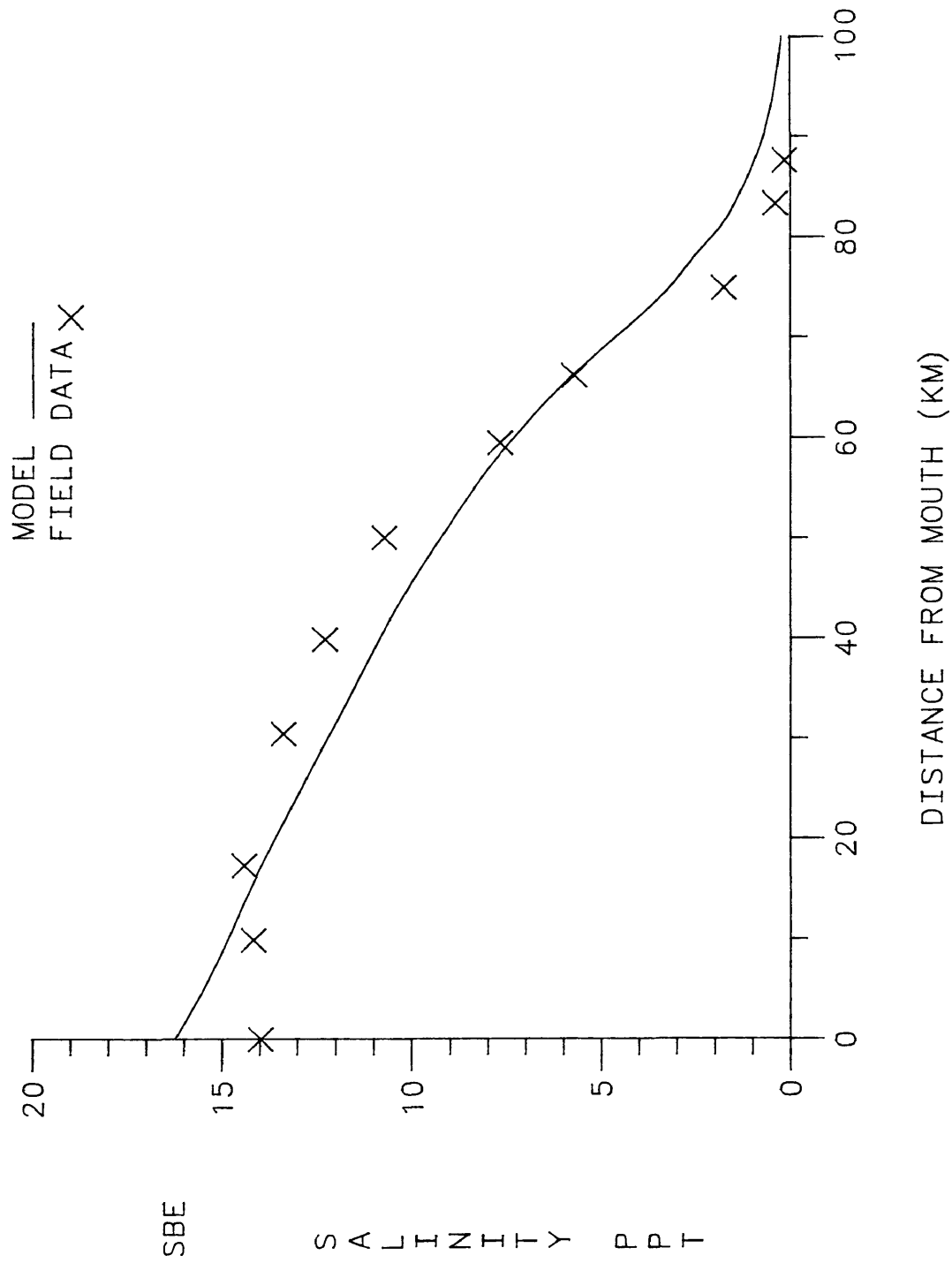
The salinity data from the intensive survey are compared to the model predictions at Windmill Point and Grey Point in Figures (4-18) and (4-19). The agreement between the predicted and measured salinity is quite good. Both records show a semi-diurnal variation in salinity. The field data shows more variability than the predicted salinity. This is expected because the model predicts the average salinity in a segment volume and the field data is measured at only one cross-section along that segment.



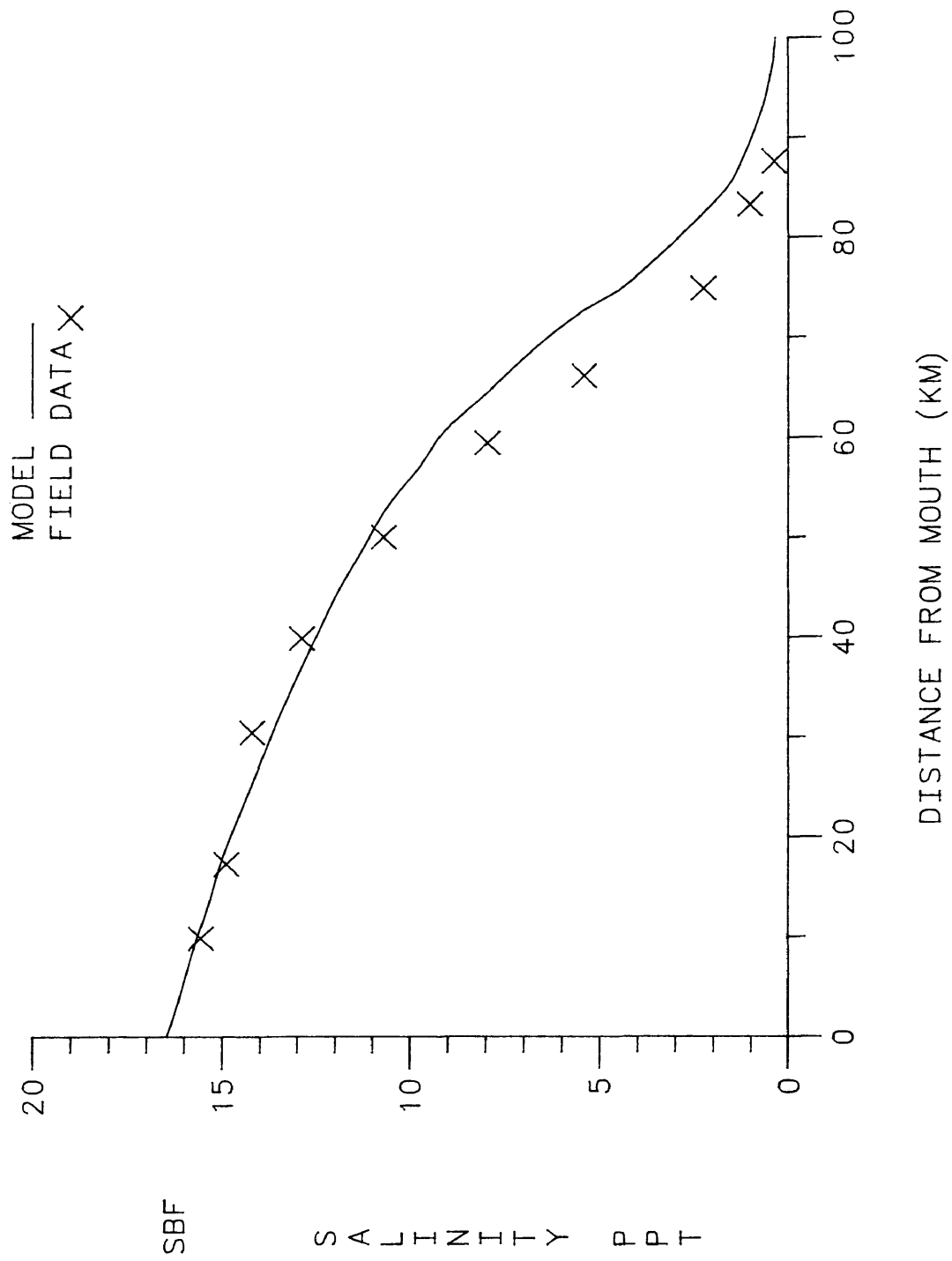
MAY 31, 73, CRUISE OSR04  
FIGURE 4-13



JUL 11, 73, CRUISE OSR05  
FIGURE 4-14

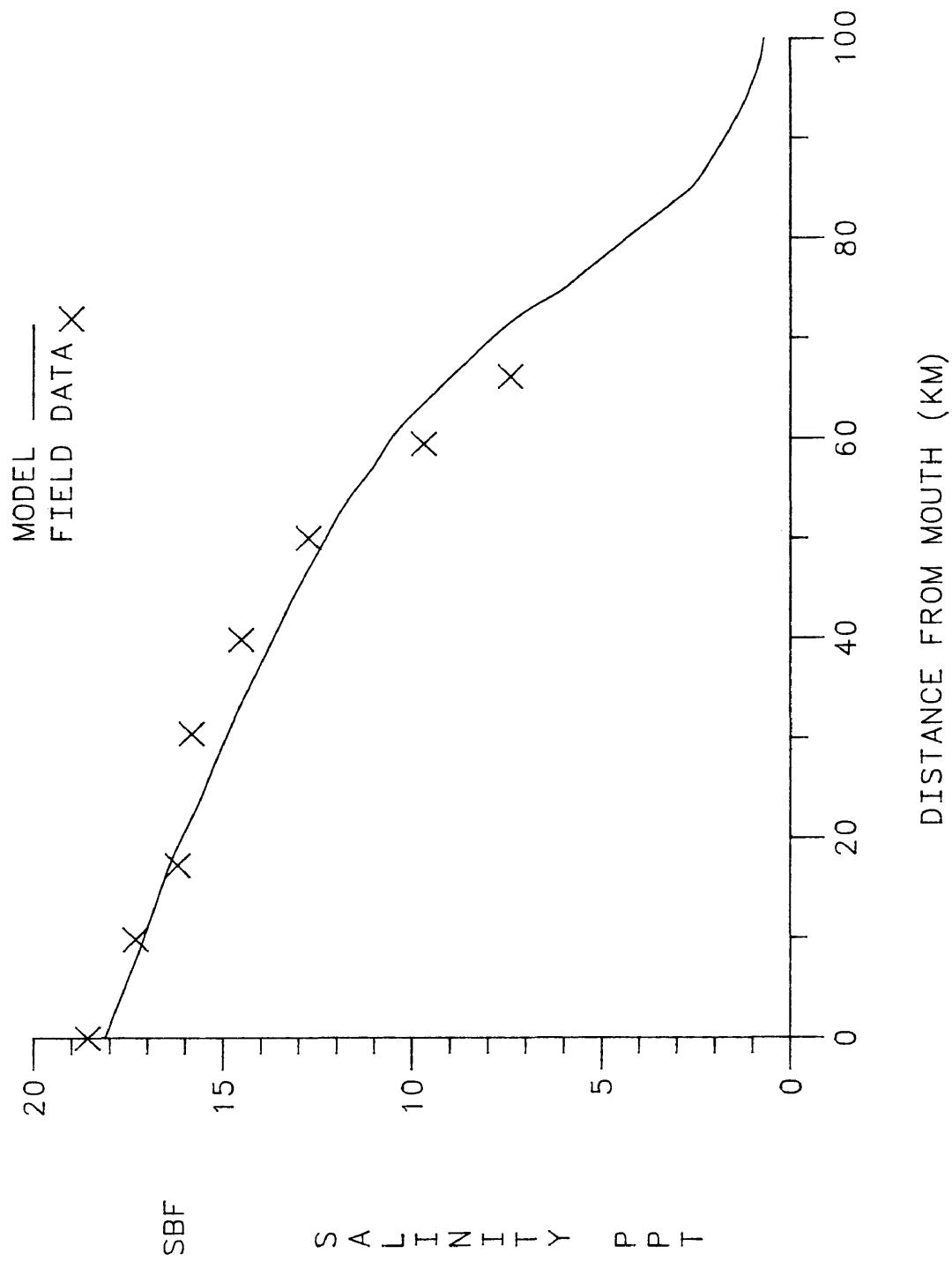


AUG 8, 73, CRUISE OSR24  
FIGURE 4-15



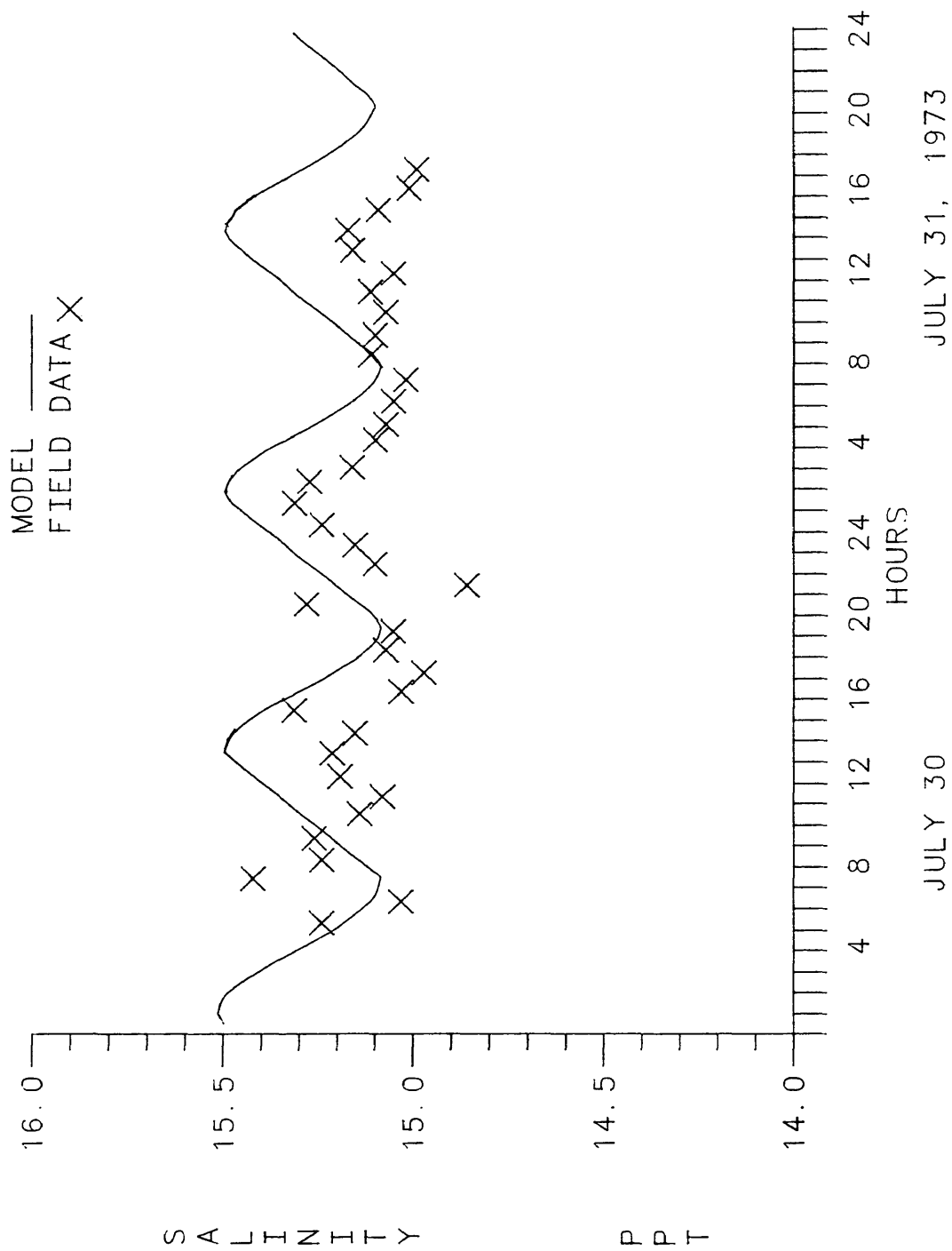
SEP 26, 73, CRUISE OSR27

FIGURE 4-16

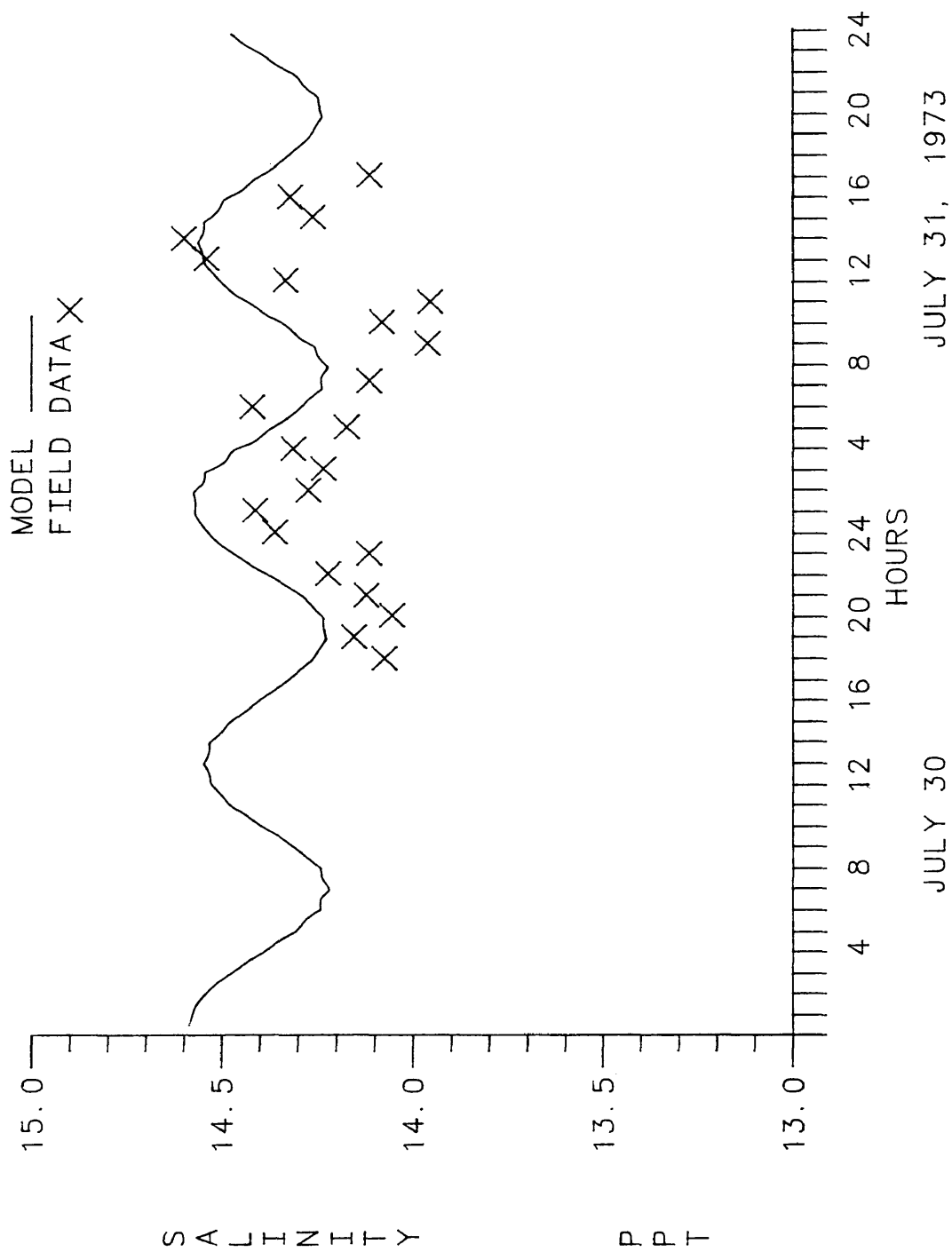


OCT 30, 73, CRUISE OSR28  
FIGURE 4-17





SALINITY AT WINDMILL POINT  
FIGURE 4-18



SALINITY AT GREY POINT  
FIGURE 4-19

#### D. The Role of Gravitational Circulation and Stratification in the Dispersion Coefficient

The importance of gravitational circulation to dispersion is evident from the values shown in Table 3. The dispersion due to gravitational flow and that due to shear flow at maximum ebb and maximum flood currents, and the total dispersion at slack tide are shown. The values shown are those calculated for July 11, 1973. The dispersion due to gravitational circulation is clearly dominant in the saline portion of the estuary. The dispersion due to gravitational flow is several orders of magnitude larger than that due to shear flow in the salinity intrusion region. It is greatest near the mouth and decreases as salinity decreases. Shear flow is the only source of dispersion in the freshwater portion of the estuary. The dispersion due to shear flow is greatest near the head where the current speed is greatest. The dispersion varies throughout the tidal cycle and is much greater at maximum current speeds than at minimum current during slack tide.

The dispersion due to gravitational circulation was formulated to depend on the longitudinal salinity gradient and the Richardson number.

$$E_G = \alpha_1 [1 + Ri]^4 \left( \frac{\delta S}{\delta x} \right)^2 \quad (3-46)$$

The Richardson,  $Ri$ , is a measure of stability. If the Richardson number is less than  $\frac{1}{4}$ , the flow becomes turbulent. Turbulence is not necessarily suppressed if  $Ri > \frac{1}{4}$ . Observations in estuaries and the open sea, indicate that turbulence exists at high values of  $Ri$ . In an estuary, if  $Ri$  is large it is expected that the estuary will be strongly stratified and gravitational flows will be dominant. If  $Ri$  is small,

the estuary will be well-mixed. Therefore as the Richardson number becomes larger, the gravitational circulation grows stronger and dispersion increases.

The Richardson number was formulated to be a function of the average cross-sectional salinity, the freshwater flow and the tidal flow.

$$Ri = \alpha_2 S \left( \frac{U_f}{\bar{U}_t} \right)^{.65} \quad (3-56)$$

It is reasonable to express the Richardson number as a function of these parameters. Estuaries are more stratified where the salinity is greatest and the stratification decreases as the salinity decreases. Estuaries become more stratified as the freshwater flow increases. An increase in tidal flow will increase turbulence and break down stratification.

Ri as defined in Equation (3-40) is difficult to measure. Pritchard (1960) formulated a general Ri that may be defined:

$$Ri = gkD \frac{\Delta S}{(.7 U)^2} \quad (4-2)$$

where  $\Delta S$  is the difference between surface and bottom salinity, and  $U$  is the average tidal velocity. Ri can be calculated using Equation (4-2),  $\Delta S$  from the slack water survey and  $U$  from the NOS Tidal Current Tables.

Table 4 displays the values of Ri as calculated in the model using Equation (3-56) where  $\alpha_2 = 5$ , and Ri as calculated from Equation (4-2) for the July slack survey.

The two sets of values for Ri are quite close with the exception of the station at the mouth. This is due to the localized well-mixed condition at the mouth. The values of Ri are higher near the mouth and

decrease upstream. This trend is expected because the estuary is more stratified where the salinity is highest and changes to well-mixed at the tail of the salinity intrusion.

TABLE 3

	DISTANCE FROM MOUTH	GRAVITATIONAL DISPERSION FLOOD	GRAVITATIONAL DISPERSION EBB	SHEAR DISPERSION FLOOD	SHEAR DISPERSION EBB	TOTAL DISPERSION SLACK
	KM	M <sup>2</sup> /SEC	M <sup>2</sup> /SEC	M <sup>2</sup> /SEC	M <sup>2</sup> /SEC	M <sup>2</sup> /SEC
2	176.51	0.00	0.00	1.00	1.00	0.00
3	173.61	0.00	0.00	1.42	559.09	1.05
4	170.23	0.00	0.00	4.13	616.57	1.09
5	167.18	0.00	0.00	17.69	991.73	1.03
6	163.64	0.00	0.00	9.84	198.90	1.05
7	160.26	0.00	0.00	10.08	151.19	1.14
8	156.56	0.00	0.00	15.12	135.07	1.04
9	153.18	0.00	0.00	17.64	145.01	1.10
10	149.15	0.00	0.00	11.05	97.22	1.11
11	145.78	0.00	0.00	32.15	178.70	1.10
12	141.91	0.00	0.00	28.98	163.91	1.00
13	138.53	0.00	0.00	8.09	27.29	1.08
14	135.16	0.00	0.00	21.94	98.44	1.13
15	130.81	0.00	0.00	13.20	43.12	1.11
16	126.79	0.00	0.00	4.71	15.56	1.10
17	123.09	0.00	0.00	18.38	65.37	1.12
18	119.87	0.00	0.00	6.34	11.63	1.22
19	116.33	0.00	0.00	50.90	71.22	1.11
20	112.15	0.00	0.00	15.64	24.95	1.27
21	107.80	0.00	0.00	6.19	9.15	1.14
22	103.94	0.00	0.00	3.27	4.19	1.02
23	99.44	0.00	0.00	21.10	40.83	1.24
24	95.57	0.00	0.00	4.67	6.99	1.03
25	91.23	0.00	0.00	2.28	2.92	1.10
26	86.89	0.01	0.00	3.88	6.63	1.31
27	83.51	0.00	0.00	2.74	4.13	1.17
28	79.65	0.00	0.00	1.98	2.49	1.51
29	76.27	0.01	0.00	2.01	2.38	3.98
30	73.85	0.03	0.01	1.89	2.09	3.07
31	70.15	0.71	0.22	1.75	1.83	16.03
32	66.13	6.86	1.42	1.78	1.81	32.85
33	62.75	215.28	89.38	1.78	1.74	41.21
34	58.25	589.96	262.11	1.60	1.59	85.64
35	55.99	604.39	650.68	1.83	1.83	55.79
36	50.84	1004.65	607.11	1.68	1.73	108.67
37	46.50	1223.87	882.49	1.86	1.96	132.34
38	41.67	1286.89	1040.51	1.80	1.92	157.96
39	37.01	1224.05	1020.53	1.87	1.97	146.18
40	31.38	1438.81	1068.16	2.39	2.53	192.42
41	25.42	1697.89	1190.49	2.95	3.15	232.67
42	20.92	1722.52	1581.65	3.56	3.81	219.77
43	14.96	1779.30	1391.83	3.13	3.31	286.01
44	11.26	1677.76	1589.33	3.27	3.47	267.65
45	5.95	2002.35	1656.26	4.01	4.13	404.27
46	1.13	1877.10	1877.57	3.04	3.16	633.03

**TABLE 4**  
**RICHARDSON NUMBERS**

<b>DISTANCE FROM MOUTH</b>	<b><math>\Delta S</math></b>	<b>Ri</b>	<b>Ri</b>
<b>KM</b>	<b>PPT</b>	<b>EQU (4-2)</b>	<b>EQU (3-56)</b>
0.0	0.45	1.2	11.8
9.8	2.14	12.3	10.4
17.2	2.61	11.9	9.2
30.4	2.90	11.8	8.1
40.0	3.87	10.3	6.8
50.0	3.51	4.5	5.2
59.5	3.54	2.2	3.4
66.1	2.68	0.3	1.0
74.8	0.10	0.1	0.2

## V. SUMMARY AND CONCLUSIONS

The objective of this study was to apply a one-dimensional, real-time, hydrodynamic and salinity intrusion model to an estuary in order to predict the longitudinal salinity distribution. It was necessary to formulate a dispersion coefficient to account for the effect of gravitational circulation in the saline portion of the estuary.

The model is based on the one-dimensional equations of conservation of volume, momentum and mass. The estuary was divided into segments and a semi-implicit finite difference scheme was used to solve the governing equations.

The dispersion coefficient was formulated to consist of three terms. The first term accounts for effects of vertical shear of the tidal current, the second accounts for effects of transverse shear of the tidal current. The third term accounts for effects of density induced circulation. The first two terms are based on Taylor's analysis of flow and are applicable in the freshwater portion of the estuary. The third term is formulated basing on the analysis of Hansen and Rattray (1965). The dispersion due to gravitational circulation is found to depend on local hydraulic conditions and the local longitudinal salinity gradient.



The model was first tested empirically by applying it to a constant cross-section channel, closed at one end. The model solution approached the analytical solution for a tidal wave propagating in such a channel.

The model was then applied to the Rappahannock River and run for hydrodynamic calibration at mean tide range. The inputs used for this calibration were a constant fresh water inflow at the head and the time-varying surface elevation at the mouth. The model reproduced the dynamics of the river quite well. The tidal range was predicted well along the river. The speed of the phases of the tidal wave were predicted adequately.

The predicted currents were compared to those measured during an intensive survey. The time varying inflow, as measured at Fredricksburg, and the predicted hourly tidal height at the mouth were the necessary boundary conditions. The comparison showed that the currents were modeled well. The predicted currents were lower than those measured because the model predicted the average current speed in a cross-section and currents were measured in the channel where current speeds are highest.

The model was calibrated for longitudinal salinity distribution using the salinity at the mouth as the additional boundary condition. The longitudinal salinity distribution was reproduced very well for a wide range of freshwater inflow rates. The model predicted salinities were lower than those measured in the middle of the salinity intrusion region and higher than those measured in the inner region of the intrusion. The predicted salinities were compared to those measured at ten stations on five slack water surveys. (Not all stations were sampled on every survey.) Of the forty-two salinity samples, the

difference between the measured and predicted values was less than 1 ppt in 32 cases or 76% of the samples. The difference was less than .5 ppt in 19 cases or 45% of the samples. If the station at the mouth was neglected, the difference was less than 1 ppt in 31 of 38 cases or 82% of the samples and less than .5 ppt in 19 cases or 50% of the samples. The agreement with the slack water survey data was quite good for the eight months simulated.

The model has been shown to be a reasonable and inexpensive method of predicting longitudinal salinity distribution over long time periods with a wide range of boundary conditions. The only inputs necessary for prediction are freshwater inflow, the surface level and salinity at the mouth.

The model is a real-time model, therefore salinity is calculated throughout the tidal cycle. This enables salinity to be presented in many ways for comparison. It may be presented as instantaneous salinities at a particular time, or at either slack water or averaged over a tidal cycle.

The one-dimensional dispersion coefficient is based on knowledge of the vertical distribution of salinity and density current. Changes in tidal amplitude and freshwater inflow change the salinity gradient and therefore the density currents, the dispersion coefficient accounts for this effect. The dispersion coefficient can be incorporated into other mass transfer models to predict distribution of dissolved substances other than salt.

### **Recommendations for Future Work**

The aim of this study was to formulate a longitudinal dispersion coefficient which incorporates the effect of gravitational circulation on dispersion. Longitudinal dispersion is also affected by secondary circulation. This circulation arises from vertical and lateral velocities produced by changes in cross-sectional form and by bends in the estuary. These flows are difficult to measure and predict. Improved measurements and understanding of these flows are necessary to formulate a dispersion coefficient which incorporates the effects of the secondary circulation.

## APPENDIX

Integration of Hansen and Rattray's similarity solutions to obtain an expression for the longitudinal dispersion coefficient for dispersion due to gravitational circulation.

### DEFINITION OF TERMS

$x, z$	Rectangular space coordinates with origin in the mean sea surface, positive seaward and downward.
$U$	Horizontal velocity component.
$g$	Gravitational acceleration.
$B, D$	Width and depth of channel.
$A_v$	Vertical turbulent viscosity.
$K_h, K_v$	Horizontal and vertical turbulent diffusivity.
$\rho, \rho_f$	Density of estuarine water and of freshwater.
$S, \Theta$	Salinity.
$\phi$	Streamfunction.
$k$	$(1/\rho_f)(\partial\rho/\partial s) = 0.00075$
$Ra$	Estuarine Rayleigh number.
$M$	Tidal-mixing parameter.
$\xi, Z$	Dimensionless space coordinates, horizontal and vertical.
$\overline{U}$	Cross-section mean velocity.
$U_f$	The freshwater velocity.
$U_t$	The root mean square tidal velocity.
$R$	The river flow discharge rate.
$\overline{S}$	Cross-section mean salinity.
$v$	Constant representing the diffusive fraction of total upstream salt flux.

Where:

Zero subscripts indicate values at  $x = 0$ .

$$U_f = \frac{R}{BD}$$

$$Ra = \frac{gkS_o D^3}{A_v K_{ho}}$$

$$M = \frac{K_v K_{ho} B^3}{R^3}$$

$$\xi = \frac{Rx}{BDK_{ho}}$$

$$Z = \frac{z}{D}$$

$$S(x, z) = S_o [v\xi + \Theta(Z)]$$

$$\frac{\partial S}{\partial x} = \frac{U_f S_o}{K_{ho}}$$

$$U = -U_f \frac{d\phi}{d\eta}$$

$$\overline{U} = U_f$$

$$S = S_o [1 + v\xi]$$

$$\frac{v Ra}{48} = \frac{1}{3} \left( \sqrt{\frac{gD\Delta\rho/\rho}{U}} \right)^{1/2}$$

The purpose is to vertically integrate Hansen and Rattray's similarity solutions to obtain an expression for the one-dimensional dispersion coefficient for dispersion due to gravitational circulation.

The advection-diffusion equation:

$$\int_0^1 U S \, dZ = US - E \frac{\delta S}{\delta x} \quad (\text{A-1})$$

The similarity solutions for horizontal velocity and salinity distribution (Hansen and Rattray 1965):

$$\frac{U}{U_f} = - \frac{d\phi}{dZ} \quad (\text{A-2})$$

$$\phi(Z) = \frac{1}{2} (2 - 3Z + Z^2) - \frac{\nu Ra}{48} (Z - 3Z^2 + 2Z^3) \quad (\text{A-3})$$

$$\frac{d\phi}{dZ} = - \frac{3}{2} + \frac{3}{2}Z^2 + \frac{\nu Ra}{48} (1 - 9Z^2 + 8Z^3) \quad (\text{A-4})$$

Substitute (A-4) into (A-2):

$$\frac{U}{U_f} = \frac{3}{2} - \frac{3}{2}Z^2 + \frac{\nu Ra}{48} (1 - 9Z^2 + 8Z^3) \quad (\text{A-5})$$

$$\frac{S}{S_0} = 1 + \nu \xi + \frac{\nu}{M} \left[ (Z - \frac{1}{2}) - \frac{1}{2}(Z^2 - \frac{1}{3}) - \int_0^Z \phi \, dZ + \int_0^1 \int_0^Z \phi \, dZ' \, dZ \right] \quad (\text{A-6})$$

$$\int_0^Z \phi \, dZ = \frac{1}{2} (2Z - \frac{3}{2}Z^2 + \frac{1}{4}Z^4) - \frac{\nu Ra}{48} (\frac{1}{2}Z^2 - \frac{3}{4}Z^4 + \frac{2}{30}Z^5) \quad (\text{A-7})$$

$$\begin{aligned} \int_0^1 \int_0^Z \phi \, dZ' \, dZ &= \frac{1}{2} (Z^2 - \frac{1}{2}Z^3 + \frac{1}{20}Z^5) - \frac{\nu Ra}{48} (\frac{1}{6}Z^3 - \frac{3}{20}Z^5 + \frac{2}{5}Z^6) \quad (\text{A-8}) \\ &= \frac{1}{2} (1 - \frac{1}{2} + \frac{1}{20}) - \frac{\nu Ra}{48} (\frac{1}{6} - \frac{3}{20} + \frac{2}{30}) \\ &= \frac{11}{40} - \frac{\nu Ra}{48} (\frac{1}{12}) \end{aligned}$$

Substitute (A-7) and (A-8) into (A-6):

$$\frac{S}{S_o} = 1 + \nu \xi + \frac{\nu}{M} \left[ \frac{1}{4} Z^2 - \frac{1}{8} Z^4 - \frac{7}{120} + \frac{\nu R_a}{48} \left( \frac{1}{2} Z^2 - \frac{3}{4} Z^4 + \frac{2}{5} Z^6 - \frac{1}{12} \right) \right] \quad (A-9)$$

Multiply (A-4) by (A-9):

$$\frac{US}{U_f S_o} = \left\{ \frac{3}{2} - \frac{3}{2} Z^2 + \frac{\nu R_a}{48} (1Z - 9Z^3 + 8Z^5) \right\} * \quad (A-10)$$

$$\left\{ 1 + \nu \xi + \frac{\nu}{M} \left[ \frac{1}{4} Z^2 - \frac{1}{8} Z^4 - \frac{7}{120} + \frac{\nu R_a}{48} \left( \frac{1}{2} Z^2 - \frac{3}{4} Z^4 + \frac{2}{5} Z^6 - \frac{1}{12} \right) \right] \right\}$$

$$\frac{US}{U_f S_o} = \left[ \frac{3}{2} - \frac{3}{2} Z^2 + \frac{\nu R_a}{48} (1 - 9Z^2 + 8Z^4) \right] \quad (A-11)$$

$$+ \nu \xi \left[ \frac{3}{2} - \frac{3}{2} Z^2 + \frac{R_a}{48} (1 - 9Z^2 + 8Z^4) \right]$$

$$+ \frac{\nu}{M} \left[ \frac{3}{8} Z^2 - \frac{3}{16} Z^4 - \frac{7}{80} + \frac{\nu R_a}{48} \left( \frac{3}{4} Z^2 - \frac{9}{8} Z^4 + \frac{3}{5} Z^6 - \frac{1}{8} \right) \right]$$

$$+ \frac{\nu}{M} \left[ -\frac{3}{8} Z^4 + \frac{3}{16} Z^6 + \frac{7}{80} Z^2 + \frac{\nu R_a}{48} \left( -\frac{3}{4} Z^4 + \frac{9}{8} Z^6 - \frac{3}{5} Z^8 + \frac{1}{8} Z^2 \right) \right]$$

$$+ \frac{\nu}{M} \left( \frac{\nu R_a}{48} \right) \left[ \frac{1}{4} Z^2 - \frac{1}{8} Z^4 - \frac{7}{120} + \frac{\nu R_a}{48} \left( \frac{1}{2} Z^2 - \frac{3}{4} Z^4 + \frac{2}{5} Z^6 - \frac{1}{12} \right) \right]$$

$$+ \frac{\nu}{M} \left( \frac{\nu R_a}{48} \right) \left[ -\frac{9}{4} Z^4 + \frac{9}{8} Z^6 + \frac{21}{40} Z^2 + \frac{\nu R_a}{48} \left( -\frac{9}{2} Z^4 + \frac{27}{4} Z^6 - \frac{18}{5} Z^8 + \frac{3}{4} Z^2 \right) \right]$$

$$+ \frac{\nu}{M} \left( \frac{\nu R_a}{48} \right) \left[ 2Z^2 - Z^4 - \frac{7}{15} Z^2 + \frac{\nu R_a}{48} (4Z^2 - 6Z^4 + \frac{16}{5} Z^6 - \frac{2}{3} Z^2) \right]$$

Integrate (A-11) from surface to bottom:

$$\begin{aligned}
 \int_0^1 \frac{US}{\bar{U}_f S_o} dZ &= \left\{ \left[ \frac{3}{2}Z - \frac{1}{2}Z^3 + \frac{\nu Ra}{48} (Z - 3Z^3 + 2Z^4) \right] \right. \\
 &+ \nu \xi \left[ \frac{3}{2}Z - \frac{1}{2}Z^3 + \frac{\nu Ra}{48} (Z - 3Z^3 + 2Z^4) \right] \\
 &+ \frac{\nu}{M} \left[ \frac{1}{8}Z^3 - \frac{3}{80}Z^5 - \frac{7}{80}Z - \frac{3}{40}Z^3 + \frac{3}{112}Z^7 + \frac{7}{240}Z^9 \right] \\
 &+ \frac{\nu}{M} \left( \frac{\nu Ra}{48} \right) \left[ \frac{1}{4}Z^3 - \frac{9}{40}Z^5 + \frac{1}{10}Z^7 - \frac{1}{8}Z - \frac{3}{20}Z^3 + \frac{9}{56}Z^7 - \frac{3}{40}Z^9 + \frac{1}{24}Z^9 \right. \\
 &\quad \left. + \frac{1}{12}Z^3 - \frac{1}{40}Z^5 - \frac{7}{120}Z - \frac{9}{20}Z^3 + \frac{9}{56}Z^7 + \frac{7}{40}Z^9 + \frac{1}{3}Z^3 - \frac{1}{8}Z^5 - \frac{7}{60}Z^7 \right] \\
 &+ \frac{\nu}{M} \left( \frac{\nu Ra}{48} \right)^2 \left[ \frac{1}{6}Z^3 - \frac{3}{20}Z^5 + \frac{2}{30}Z^7 - \frac{1}{12}Z - \frac{9}{10}Z^3 + \frac{27}{28}Z^7 - \frac{18}{40}Z^9 + \frac{1}{4}Z^9 \right. \\
 &\quad \left. + \frac{2}{3}Z^3 - \frac{3}{4}Z^5 + \frac{16}{45}Z^7 - \frac{1}{6}Z^9 \right] \Bigg\}_0^1
 \end{aligned} \tag{A-12}$$

Combine terms:

$$\begin{aligned}
 \int_0^1 \frac{US}{\bar{U}_f S_o} dZ &= \frac{3}{2} - \frac{1}{2} + \frac{\nu Ra}{48} (1-3+2) + \nu \xi \left[ \frac{3}{2} - \frac{1}{2} + \frac{\nu Ra}{48} (1-3+2) \right] \\
 &+ \frac{\nu}{M} \left[ \frac{1}{8} - \frac{3}{80} - \frac{7}{80} - \frac{3}{40} + \frac{3}{112} + \frac{7}{240} \right] \\
 &+ \frac{\nu}{M} \left( \frac{\nu Ra}{48} \right) \left[ \frac{1}{4} - \frac{9}{40} + \frac{1}{10} - \frac{1}{8} - \frac{3}{20} + \frac{9}{56} - \frac{3}{40} + \frac{1}{24} + \frac{1}{12} - \frac{1}{40} - \frac{7}{120} \right. \\
 &\quad \left. - \frac{9}{20} + \frac{9}{56} + \frac{7}{40} + \frac{1}{3} - \frac{1}{8} - \frac{7}{60} \right] \\
 &+ \frac{\nu}{M} \left( \frac{\nu Ra}{48} \right)^2 \left[ \frac{1}{6} - \frac{3}{20} + \frac{2}{30} - \frac{1}{12} - \frac{9}{10} + \frac{27}{28} - \frac{18}{40} + \frac{1}{4} + \frac{2}{3} - \frac{3}{4} + \frac{16}{45} - \frac{1}{6} \right] \\
 &= 1 + \nu \xi + \frac{\nu}{M} \left[ -\frac{2}{105} - \frac{19}{420} \left( \frac{\nu Ra}{48} \right) - \frac{19}{630} \left( \frac{\nu Ra}{48} \right)^2 \right]
 \end{aligned} \tag{A-13}$$



Multiply both sides by  $U_f S_o$ :

$$\int_0^1 US \, dZ = U_f S_o [1 + v\xi] - U_f S_o \frac{v}{M} \left[ \frac{2}{105} + \frac{19}{420} \left( \frac{vRa}{48} \right) + \frac{19}{630} \left( \frac{vRa}{48} \right)^2 \right] \quad (A-14)$$

Substitute definitions for  $M$ ,  $U_f$ ,  $S_o$ :

$$\int_0^1 US \, dZ = US - \frac{\partial S}{\partial X} \left( \frac{U^2 D^2}{K_v} \right) \left[ \frac{2}{105} + \frac{19}{420} \left( \frac{vRa}{48} \right) + \frac{19}{630} \left( \frac{vRa}{48} \right)^2 \right] \quad (A-15)$$

(A-15) becomes the convection-diffusion equation:

$$\int_0^1 US \, dZ = US - E \frac{\partial S}{\partial X} \quad (A-1)$$

Therefore:

$$E = \frac{U^2 D^2}{K_v} \left[ \frac{2}{105} + \frac{19}{420} \left( \frac{\sqrt{g D \Delta \rho / \rho}}{U} \right)^{\frac{1}{2}} + \frac{19}{630} \left( \frac{\sqrt{g D \Delta \rho / \rho}}{U} \right)^{\frac{1}{2}} \right] \quad (A-16)$$

$$E = \frac{U^2 D^2}{K_v} \left[ \frac{2}{105} + \frac{19}{420} \left( \frac{vRa}{48} \right) + \frac{19}{630} \left( \frac{vRa}{48} \right)^2 \right] \quad (A-17)$$

From Hansen and Rattray's figure 4 (1965)  $\frac{vRa}{48}$  is of order 10 or larger for Virginia estuaries. Therefore the third term on the right in equation (A-17) dominates the other terms. Let:

$$E \approx \frac{19}{630} \left( \frac{1}{48} \right)^2 \left( \frac{U^2 D^2}{K_v} \right) (vRa)^2 \quad (A-18)$$

$$\approx \frac{19}{630} \left( \frac{1}{48} \right)^2 \left( \frac{g^2 k^2 D^2}{K_v A^2} \right) \left( \frac{\delta S}{\delta x} \right)^2 \quad (A-19)$$

$$E \approx 7.1 \times 10^{-10} \left( \frac{D^*}{K_v A_v} \right) \left( \frac{\delta s}{\delta x} \right)^2$$

(A-20)

#### REFERENCES CITED

- Aris, R., (1956). **On the Dispersion of a Solute Flowing Through a Tube.** Proceedings Royal Society London (A), 235, pp. 67-77.
- Arons, A. B. and Stommel, H. (1951). **A Mixing Length Theory of Tidal Flushing.** Transactions of the American Geophysical Union , Vol. 32, pp. 1986-2001.
- Blumberg, A. F. (1975). **A Numerical Model of Estuarine Circulation.** J of the Hydraulics Division, ASCE, Vol 103, pp. 295-310
- Boicourt, W. (1969). **A Numerical Model of the Salinity Distribution in Upper Chesapeake Bay.** Technical Report 54. Chesapeake Bay Institute, Johns Hopkins University.
- Boon, J. D., Kiley, K. P. (1978). **Harmonic Analysis and Tidal Prediction by the Method of Least Squares.** Va. Inst. of Marine Science, Gloucester Pt, VA., Special Report 186.
- Bowden, K. F. and Hamilton, P. (1975). **Some Experiments with a Numerical Model of Circulation and Mixing in a Tidal Estuary.** Estuarine and Coastal Marine Science, Vol. 3, pp. 281-301.
- Cerco, C. F. (1982). **Two-Dimensional, Intratidal Model Study of Salinity Intrusion and Motion in Partially-Mixed Estuaries.** Dissertation. Va. Inst. of Marine Science, College of William and Mary in Virginia.
- Dyer, K. R. and Taylor, P. A. (1973). **A Simple Segmented Prism Model of Tidal Mixing in Well-Mixed Estuaries.** Estuarine and Coastal Marine Science, Vol. 1, pp. 411-418.
- Elder, J. W. (1959). **The Dispersion of Marked Fluid in Turbulent Shear Flow.** J. of Fluid Mechanics, Vol. 5, Part 4, May 1959, pp. 554-560.
- Elliot, A. J. (1976). **A Numerical Model of the Internal Circulation in a Branching Estuary.** Chesapeake Bay Institute Special Rept. 54. The Johns Hopkins Univsersity.

- Festa J. F. and Hansen, D. V. (1976). **A Two-Dimensional Numerical Model of Estuarine Circulation: The Effects of Altering Depth and River Discharge.** *Estuarine and Coastal Marine Science*, Vol. 4, pp. 309-323.
- Fischer, H. B. (1966). **Longitudinal Dispersion in Laboratory and Natural Streams.** Thesis, California Institute of Technology at Pasadena, CA.
- Fischer, H. B. (1967). **The Mechanics of Dispersion in Natural Streams.** *J. of the Hydraulics Division, ASCE*, Vol. 93, No HY6, Nov 1967, pp. 187-216.
- Fischer, H. B. (1969). **The Effects of Bends on Dispersion in Streams.** *Water Resources Research*. Vol. 5, No 2, April 1969, pp. 496-506.
- Fischer, H. B., List, E. J., Koh, R. C. Y., Imberger J., Brooks, N. H. (1979). **Mixing in Inland and Coastal Waters.** Academic Press, N.Y.
- Hamilton, P. (1975). **A Numerical Model of the Vertical Circulation of Tidal Estuaries and its Application to the Rotterdam Waterway.** *Geophys. J. R. Astr. Soc.* Vol. 40, pp. 1-21
- Hamilton, P. (1977). **'On the Numerical Formulation of a Time-Dependent Multi-Level Model of an Estuary with Particular Reference to Boundary Conditions'.** *Estuarine Processes Vol II.* Academic Press, N. Y.
- Hansen, D. V. and Rattray, M. (1965). **Gravitational Circulation in Straits and Estuaries.** *J. of Marine Research*, Vol. 23, pp. 104-122.
- Hansen, D. V. and Rattray, M. (1966). **New Dimensions in Estuarine Classification.** *Limnology and Oceanography*, Vol. 11, pp. 319-325.
- Harleman, D. R. F. (1966). **'Diffusion Processes in Stratified Flow.'** Chap. 12. *Estuary and Coastline Hydrodynamics.* A. T. Ippen Ed., McGraw-Hill.
- Harleman, D. R. F. (1971). **One-Dimensional Models.** *Estuarine Modeling: an Assessment.* EPA 16070 DZV 02/71.
- Harleman, D. R. F. and Lee, C. H. (1969). **The Computation of Tides and Currents in Estuaries and Canals.** Technical Bulletin no. 16. Committee on Tidal Hydraulics, Army Corps of Engineers.
- Hayward, D., Welch, C. S. and Haas, L. W. (1982). **York River Destratification: an Estuary-Subestuary Interaction.** *Science*, Vol. 216, p. 1414.
- Holley, E. R. and Harleman, D. R. F. (1965). **Dispersion of Pollutants in Estuary Type Flows.** Tech. Rept. No. 74, Hydraulics Lab, MIT.

- Holley, E. R., Harleman, D. R. F. and Fischer, H. B. (1970). **Dispersion in Homogeneous Estuary Flow**. J. of the Hydraulics Division, ASCE, Vol. 96, No HY8, pp. 1691-1709.
- Ippen A. T. (1966). **'Tidal Dynamics in Estuaries: Part I, Estuaries of Rectangular Section.'** Estuary and Coastline Hydrodynamics. A. T. Ippen ed.
- Kent, R. E. and Pritchard, D. W. (1959). **A Test of Mixing Length Theories in a Coastal Plain Estuary**. J of Marine Research, Vol 18, pp. 62-72.
- Ketchum, B. H. (1951). **The Exchanges of Fresh and Salt Waters In Tidal Estuaries**. J. of Marine Research, Vol. X, pp. 18-38.
- Knudson M. (1901). **Hydrographical Tables**. Bianco Luno, Second edition 1931.
- Kuo, A. Y. (1976). **A Model of Tidal Flushing for Small Coastal Basins**. Proc. of the Conference on Environmental Modeling and Simulation. EPA 600/9-76-016, July 1976, USEPA, Washington, D.C.
- Kuo, A. Y., Nichols M., and Lewis J. (1978). **Modeling Sediment Movement in the Turbidity Maximum of an Estuary**. VPI-VWRRC Bulletin 111.
- Leendertse, J. J. (1970). **A Water-Quality Simulation Model for Well-Mixed Estuaries and Coastal Seas**. The Rand Corporation, Santa Monica, CA.
- Officer, C. B. (1976). **Physical Oceanography of Estuaries (and Associated Coastal Waters)**. John Wiley and Sons, New York.
- Okubo, A. (1964). **'Equations Describing the Diffusion of an Introduced Pollutant in a One-Dimensional Estuary.'** Studies on Oceanography. ed. K. Yosida. University of Washington Press, Seattle.
- Pritchard, D. W. (1952). **Salinity Distribution and Circulation in the Chesapeake Bay Estuarine System**. Journal of Marine Research, 11 No 2.
- Pritchard, D. W. (1954). **A Study of the Salt Balance in a Coastal Plain Estuary**. J. of Marine Research, Vol. 15, pp. 33-42
- Pritchard, D. W. (1959). **Computation of the Longitudinal Salinity Distribution in the Delaware Estuary for Various Degrees of River Inflow Regulation**. Technical Report XVIII, Chesapeake Bay Institute, Johns Hopkins University.
- Pritchard, D. W. (1960). **'The Movement and Mixing of Contaminants in Tidal Estuaries.'** Proceedings of the First International Conference on Waste Disposal in the Marine Environment, ed. E. A. Pearson, Pergamon Press, New York.

- Schureman, P. (1958). **Manual of Harmonic Analysis and Prediction of Tides.** Special Pub. No. 98, Revised 1940 Ed., reprinted 1958 with corrections, U.S. Dept. of Commerce, Coast and Geodetic Survey, Wash., D.C.
- Seitz, R. C. (1971). **Drainage Area Statistics for the Chesapeake Bay Freshwater Drainage Basin.** CBI. Special Rept. 19.
- Taylor, G. I. (1954). **The Dispersion of Matter in Turbulent Flow Through a Pipe.** Proceedings of the Royal Society of London, A 223, pp. 446-468.
- Thatcher, M. and Harleman, D. R. F. (1972). **A Mathematical Model for the Prediction of Unsteady Salinity Intrusion in Estuaries.** R. M. Parsons Laboratory, Rept. no. 144. M I T, Cambridge, Mass.
- Wang, D. P. (1983). **Two-Dimensional Branching Salt Intrusion Model.** J. of Waterway, Port, Coastal and Ocean Engineering, ASCE, Vol. 109, pp. 103-107.
- Wang, D. P. and Kravitz, D. W. (1980). **A Semi-Implicit Two-Dimensional Model of Estuarine Circulation.** J. of Physical Oceanography, Vol. 10, pp. 441-454.
- Ward, P. R. B. (1976). **Measurements of Estuary Dispersion Coefficient.** J. of the Environmental Engineering Division, ASCE, Vol 102, pp. 855-859.
- Williams, S. A. (1983). **A Mathematical Model for Small Tidal Streams Capable of Simulating Both Short-Term and Long-Term Water Quality Variations.** Thesis. Virginia Institute of Marine Science, College of William and Mary in Virginia.
- Williams, S. A. and Kuo, A. Y. (1984). **Water Quality Studies of Little Hunting Creek.** Special Report No. 268. Virginia Institute of Marine Science, College of William and Mary.
- Wood, T. (1979). **A Modification of Existing Simple Segmented Tidal Prism Models of Mixing in Estuaries.** Estuarine, Coastal and Marine Science, Vol 8, pp. 339-347.

## **VITA**

**ANNE CATHERINE WILBER**

**Born in Charlotte, North Carolina, 25 April 1953. Graduated East Mecklenburg High School in 1971. Earned B.S. in Physics from the University of North Carolina at Charlotte in 1977. Entered masters program in College of William and Mary, School of Marine Science in 1977.**